Supporting Information

(Aminoalkyl)diphenylphosphine sulfides: synthesis and application as building blocks in the design of multidentate ligands for cytotoxic Pd(II) complexes

Aleksandr V. Konovalov,[a,b] Svetlana G. Churusova,[a] Diana V. Aleksanyan,[a,c]* Ekaterina Yu. Rybalkina,[d] Svetlana A. Aksenova,[a,e] Alexander S. Peregudov,[a] Zinaida S. Klemenkova,[a] and Vladimir A. Kozlov[a]

[a] *A. N. Nesmeyanov Institute of Organoelement Compounds, Russian Academy of Sciences, ul. Vavilova 28, str. 1, Moscow, 119334 Russia*

[b] *Russian University of Chemical Technology, Miusskaya pl. 9, Moscow, 125047 Russia*

[c] *Scientific Laboratory "Advanced Composite Materials and Technologies", Plekhanov Russian University of Economics, Stremyannyi per. 36, Moscow, 117997 Russia*

[d] *N. N. Blokhin National Medical Research Center of Oncology of the Ministry of Health of the Russian Federation, Kashirskoe shosse 23, Moscow, 115478 Russia*

[e] *Moscow Institute of Physics and Technology (National Research University), Institutskiy per. 9, Dolgoprudny, Moscow Region, 141700 Russia*

*corresponding author: aleksanyan.diana@ineos.ac.ru

Table of contents

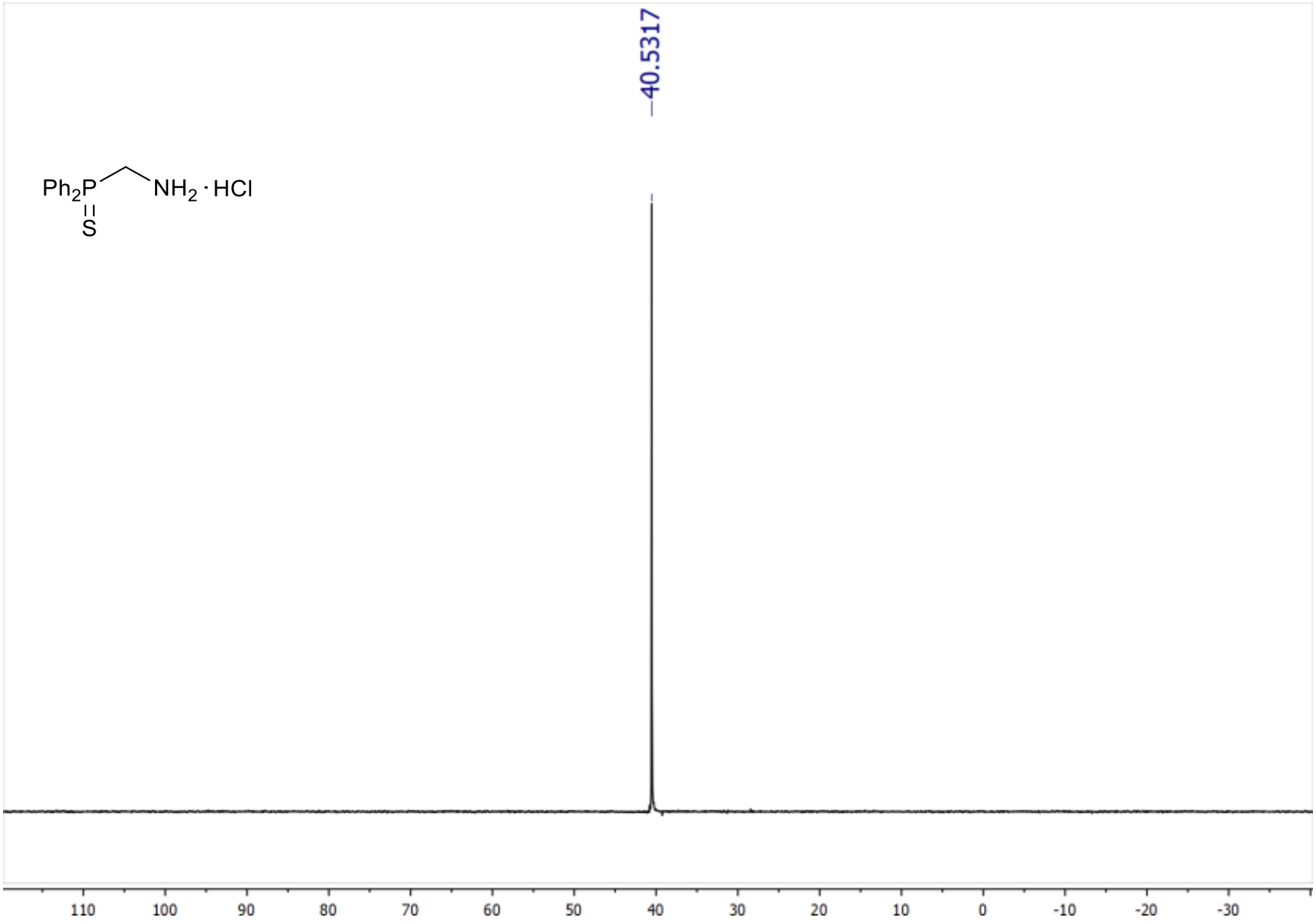

Figure S1. $^{31}P\{^{1}H\}$ NMR spectrum of (aminomethyl)diphenylphosphine sulfide hydrochloride **3** (161.98 MHz, $CDCl_3$)

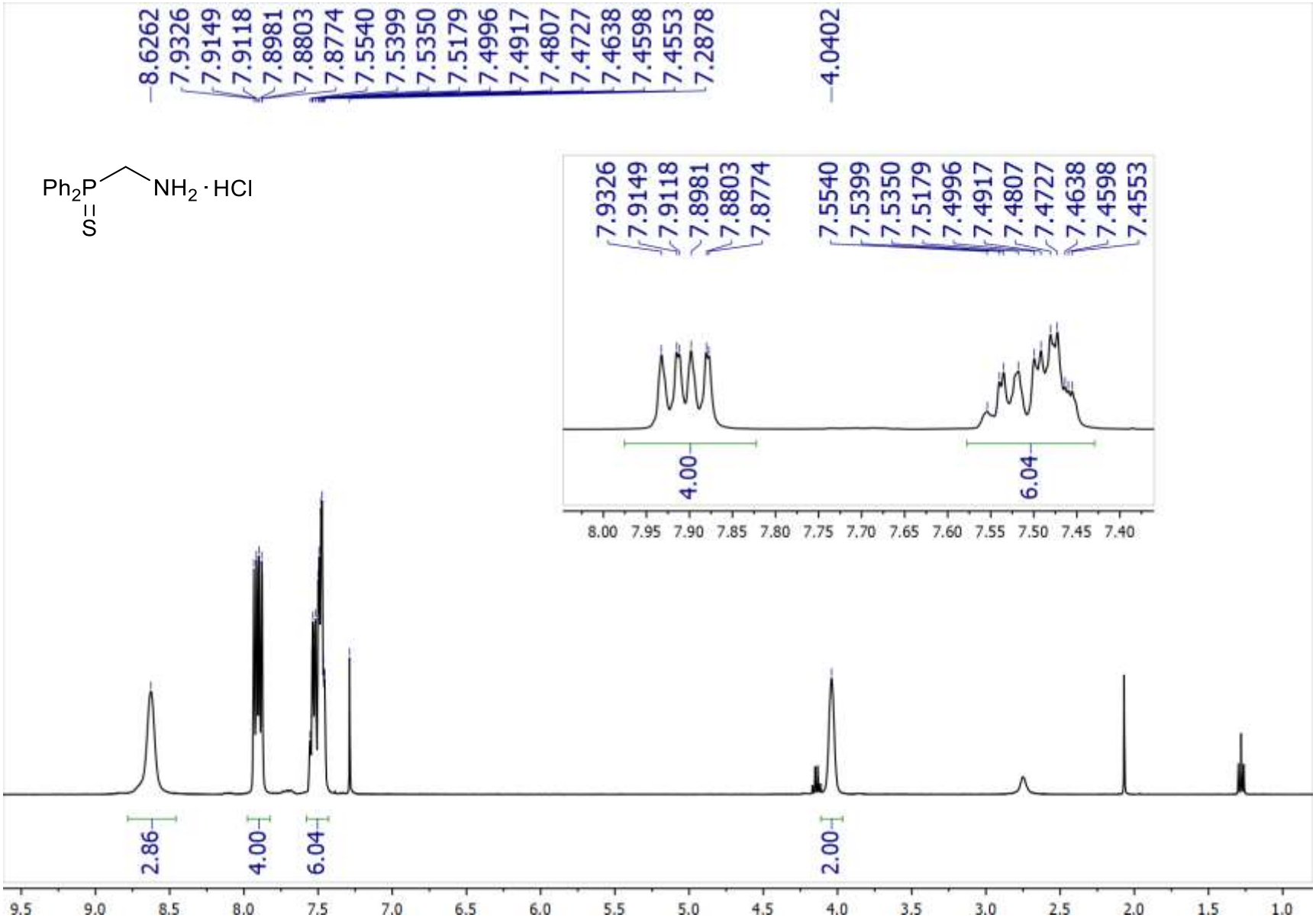

Figure S2. ^{1}H NMR spectrum of (aminomethyl)diphenylphosphine sulfide hydrochloride **3** (400.13 MHz, $CDCl_3$)

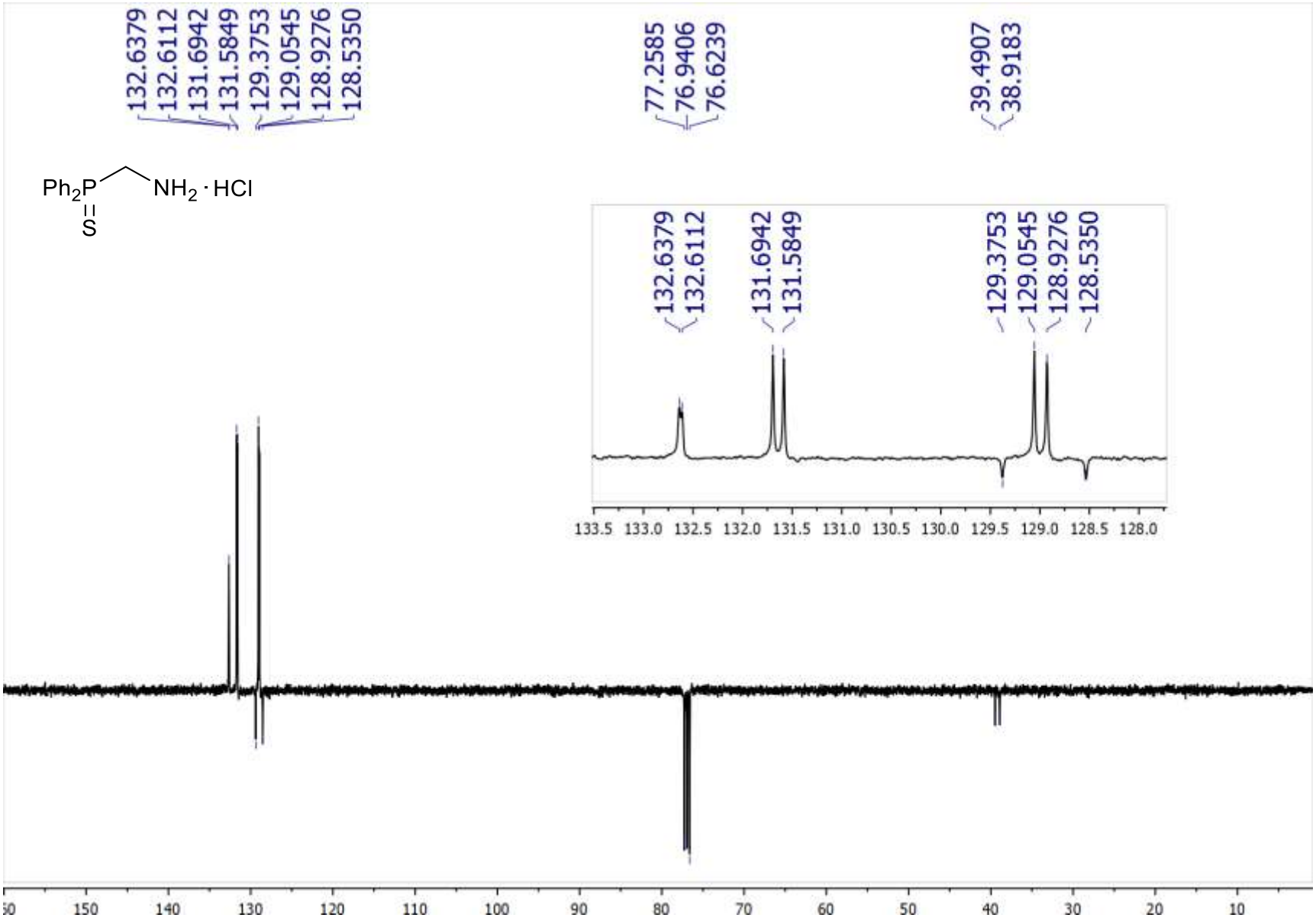

Figure S3. $^{13}C\{^{1}H\}$ NMR spectrum of (aminomethyl)diphenylphosphine sulfide hydrochloride **3** (100.61 MHz, $CDCl_3$)

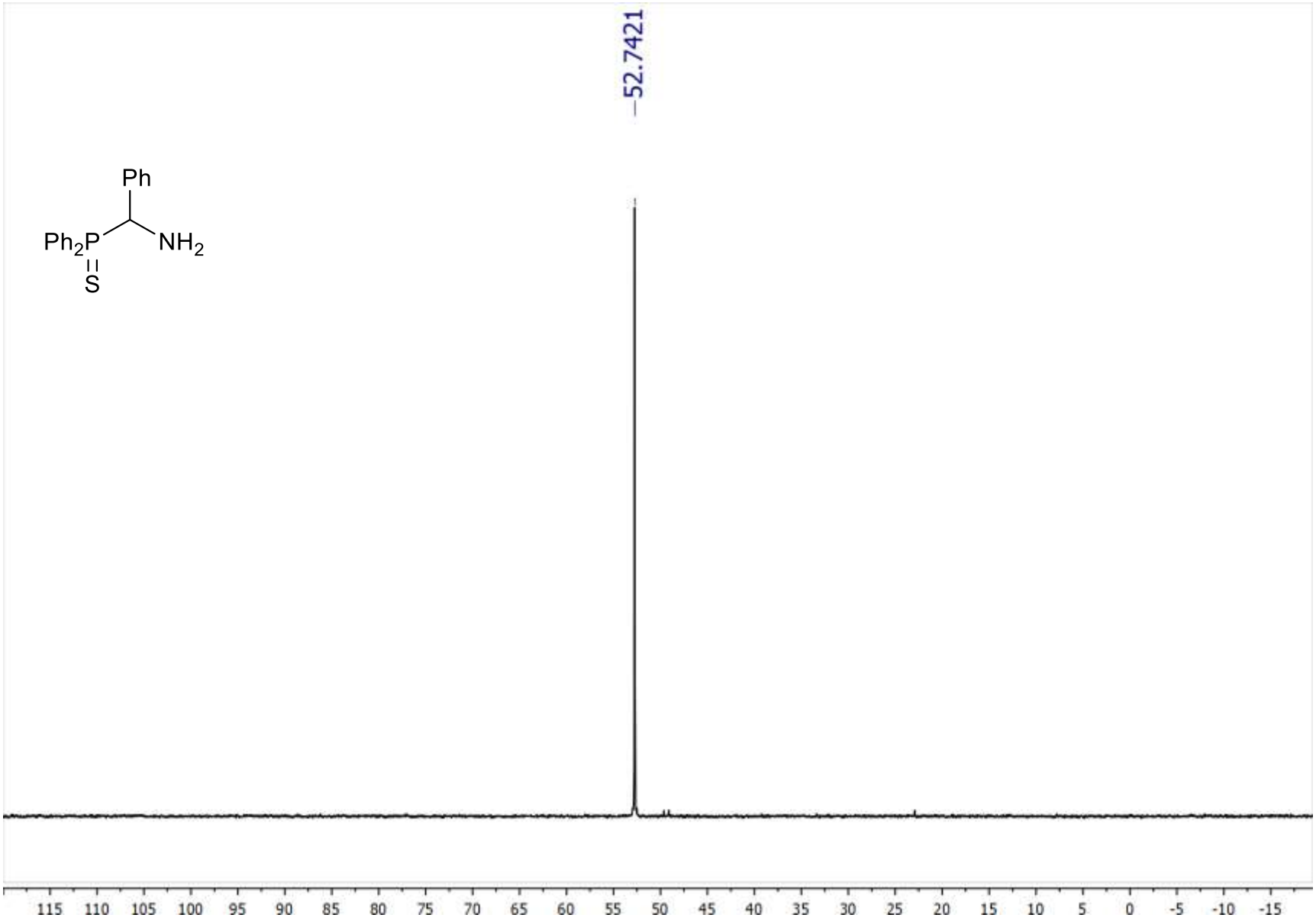

Figure S4. $^{31}P\{^{1}H\}$ NMR spectrum of [amino(phenyl)methyl]diphenylphosphine sulfide **4a** (161.98 MHz, $CDCl_3$)

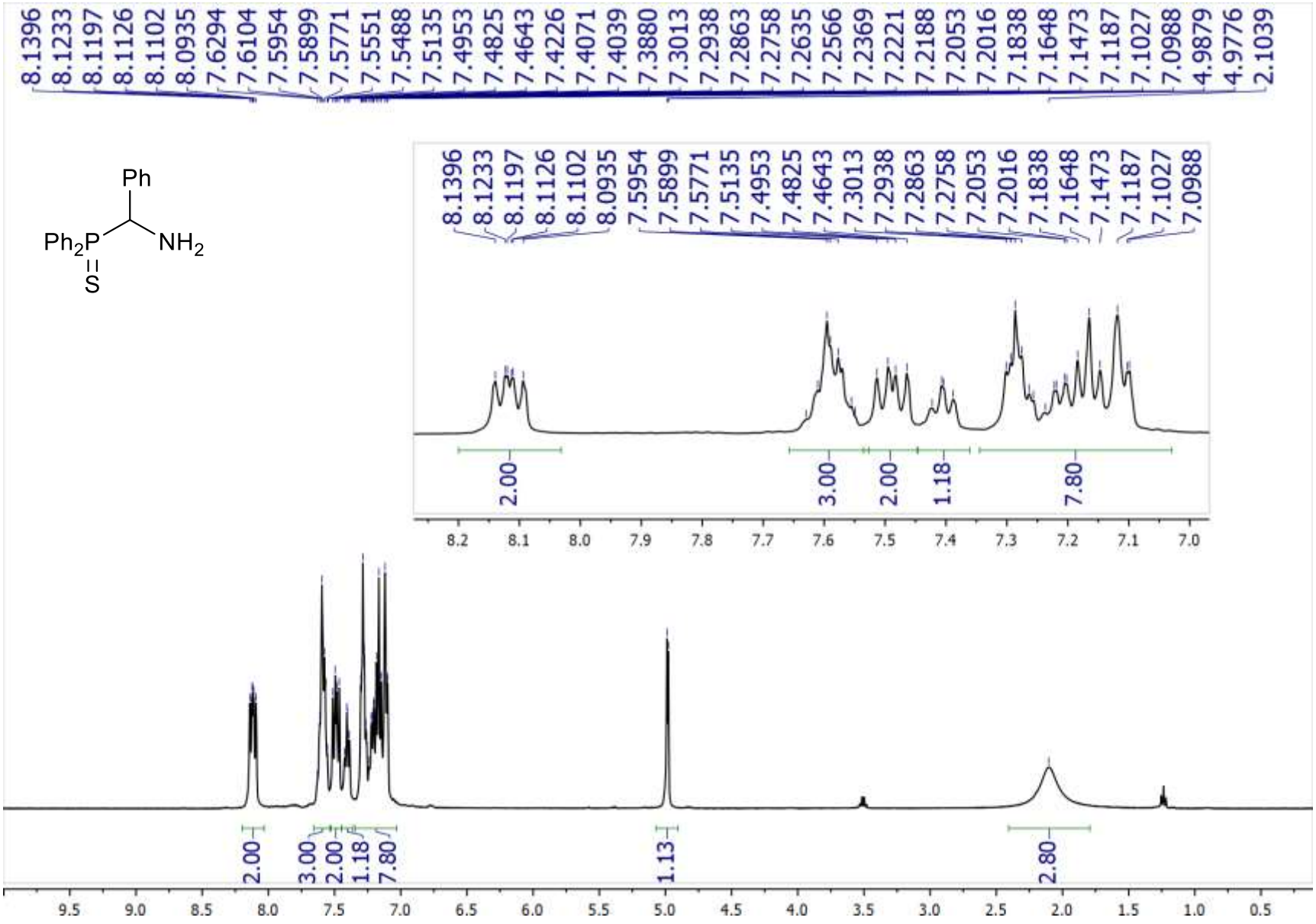

Figure S5. ^{1}H NMR spectrum of [amino(phenyl)methyl]diphenylphosphine sulfide **4a** (400.13 MHz, $CDCl_3$)

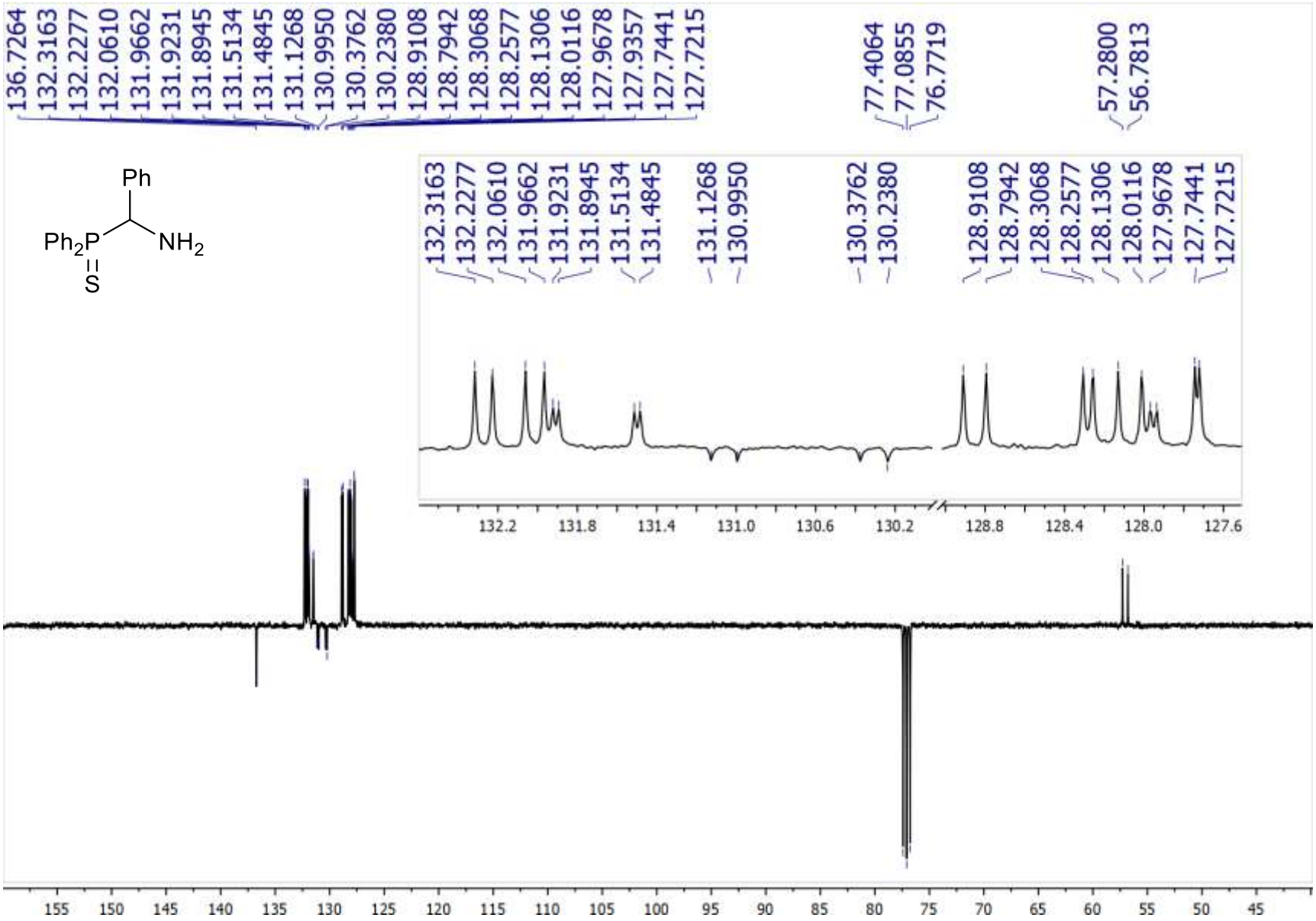

Figure S6. $^{13}C\{^{1}H\}$ NMR spectrum of [amino(phenyl)methyl]diphenylphosphine sulfide **4a** (100.61 MHz, $CDCl_3$)

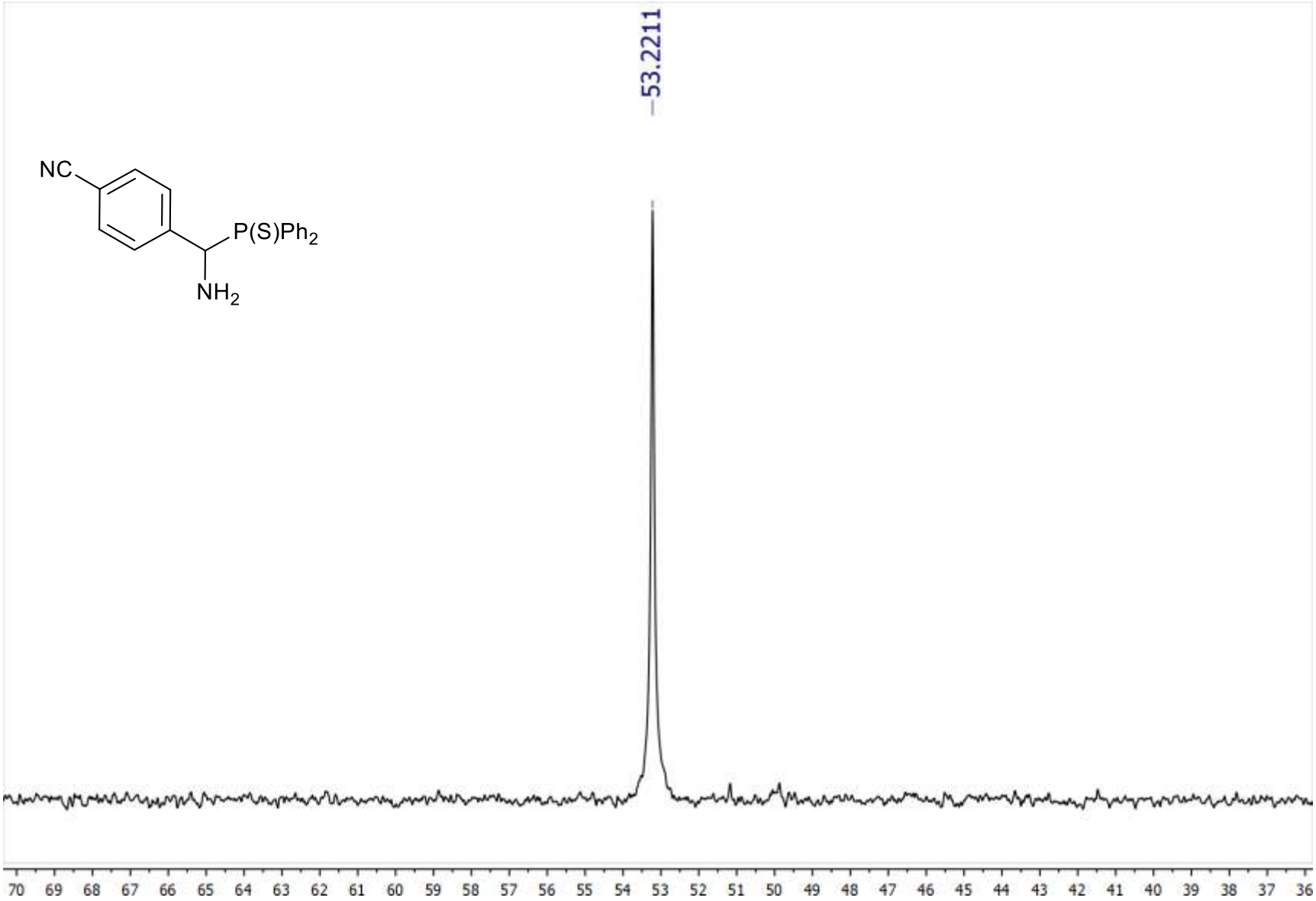

Figure S7. $^{31}P\{^{1}H\}$ NMR spectrum of 4-[amino(diphenylthiophosphoryl)methyl]benzonitrile **4c** (121.49 MHz, $CDCl_3$)

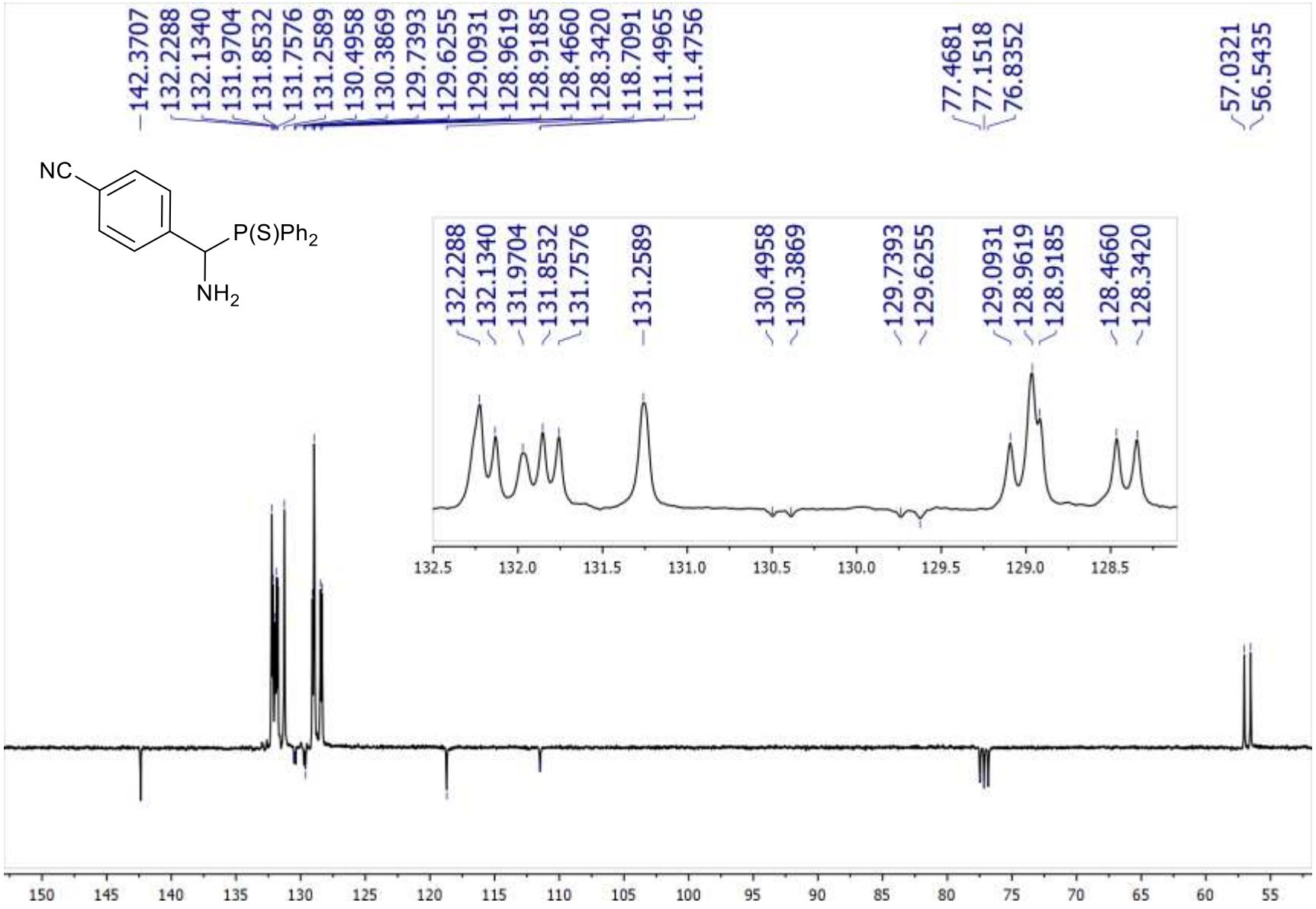

Figure S8. $^{13}C\{^{1}H\}$ NMR spectrum of 4-[amino(diphenylthiophosphoryl)methyl]benzonitrile **4c** (100.61 MHz, $CDCl_3$)

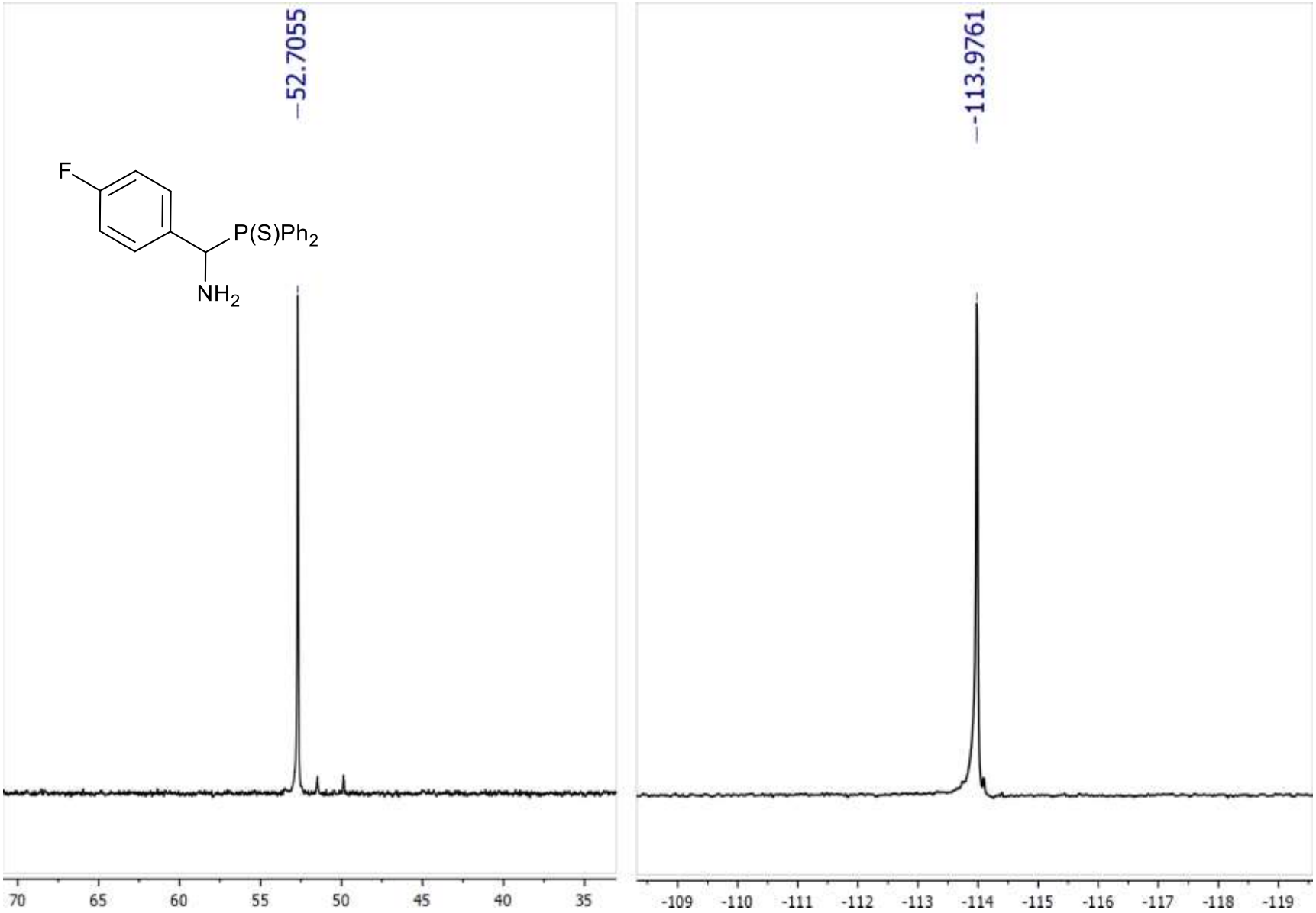

Figure S9. $^{31}P\{^{1}H\}$ (left) (161.98 MHz, $CDCl_3$) and $^{19}F\{^{1}H\}$ (right) (376.49 MHz, $CDCl_3$) NMR spectra of [amino(4-fluorophenyl)methyl]diphenylphosphine sulfide **4d**

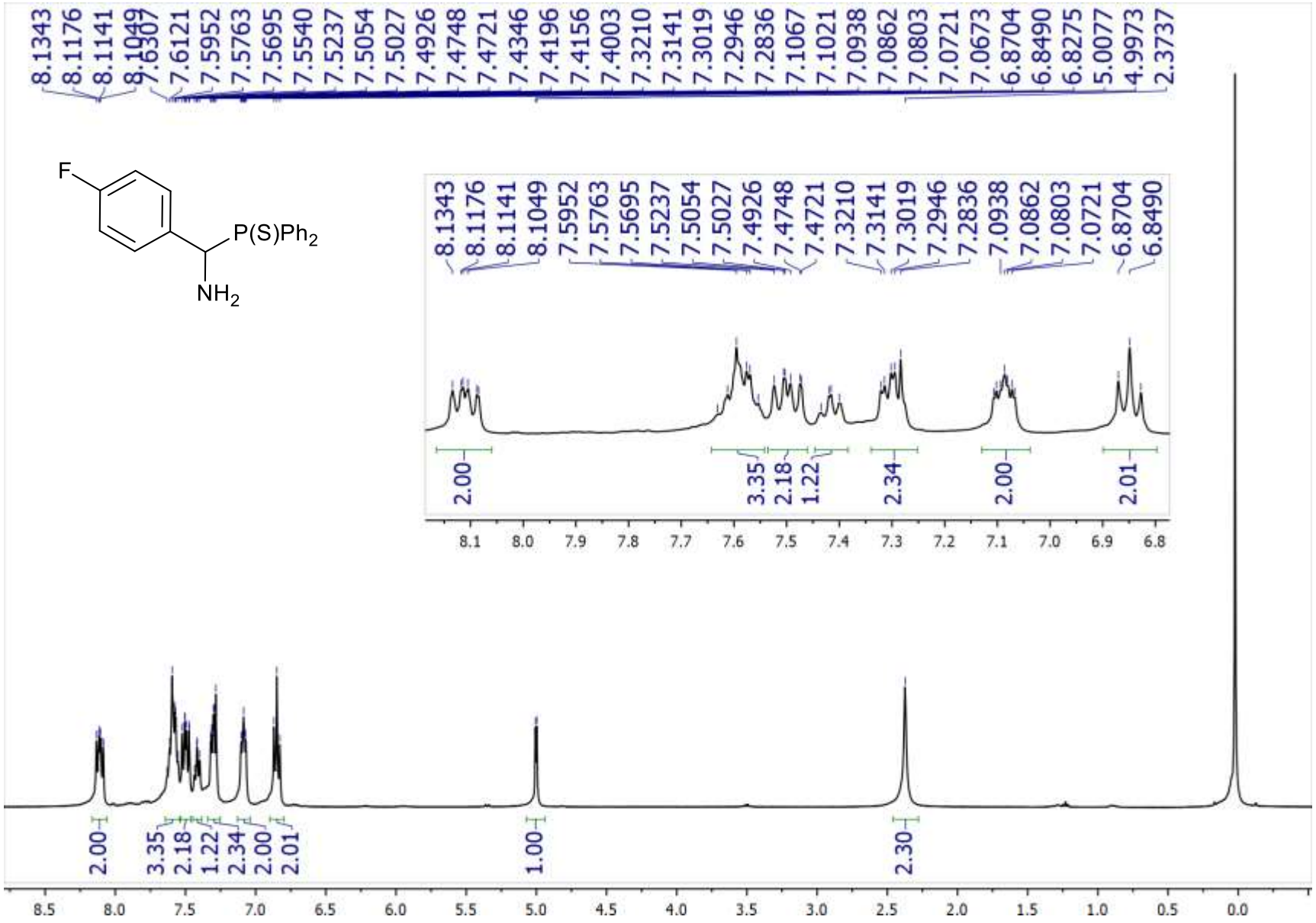

Figure S10. ^{1}H NMR spectrum of [amino(4-fluorophenyl)methyl]diphenylphosphine sulfide **4d** (400.13 MHz, $CDCl_3$)

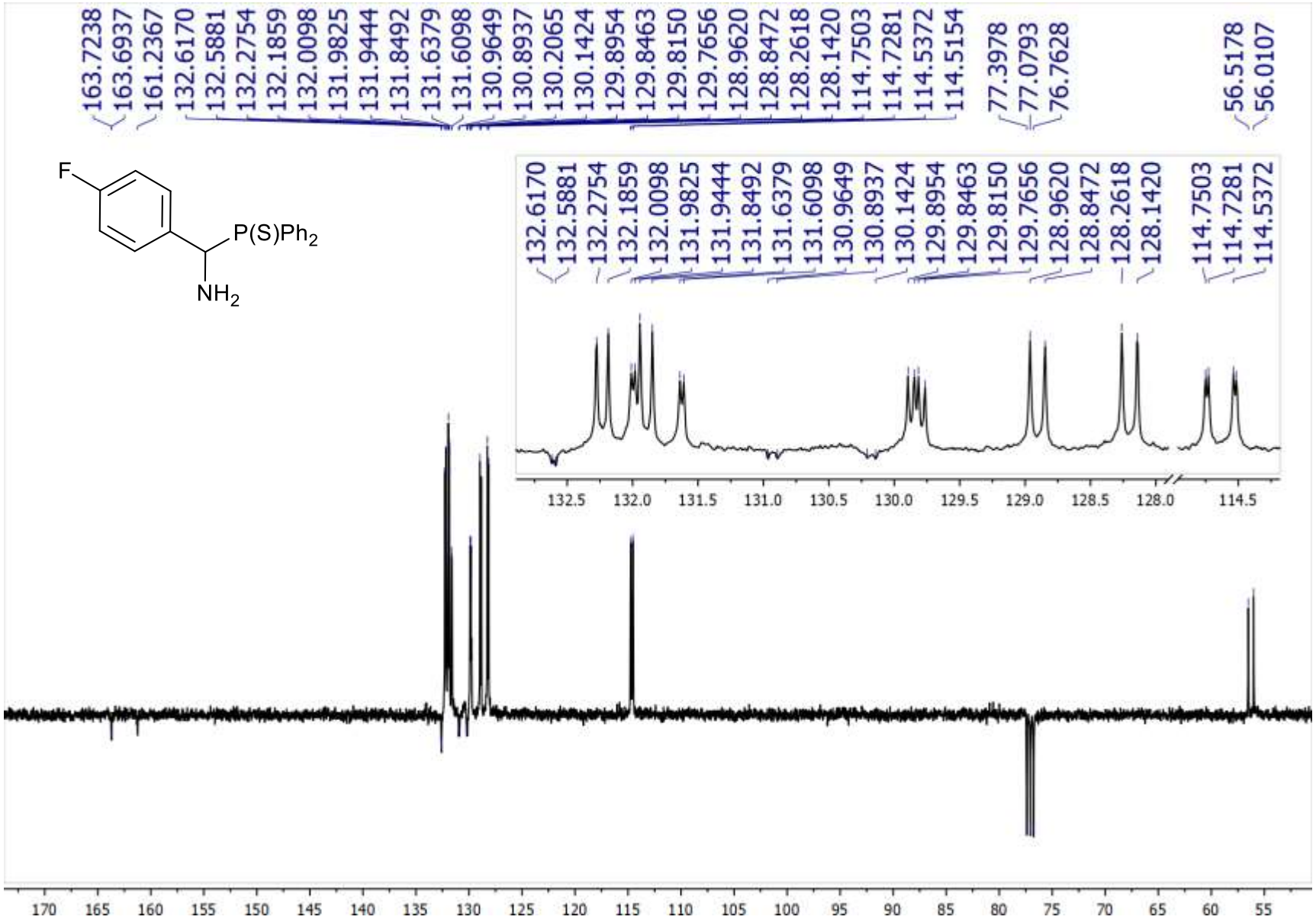

Figure S11. $^{13}C\{^{1}H\}$ NMR spectrum of [amino(4-fluorophenyl)methyl]diphenylphosphine sulfide **4d** (100.61 MHz, $CDCl_3$)

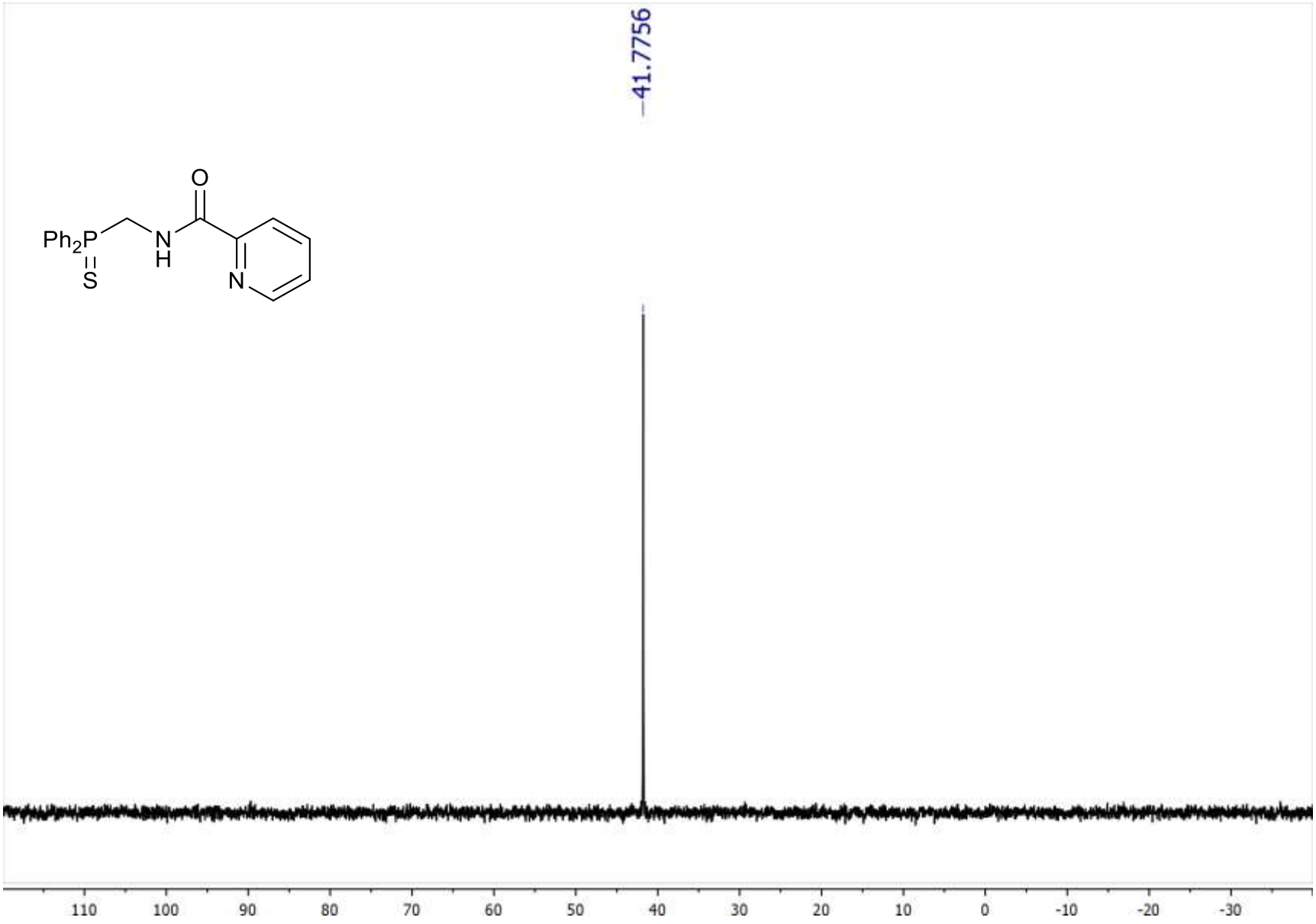

Figure S12. $^{31}P\{^{1}H\}$ NMR spectrum of ligand **5** (161.98 MHz, $CDCl_3$)

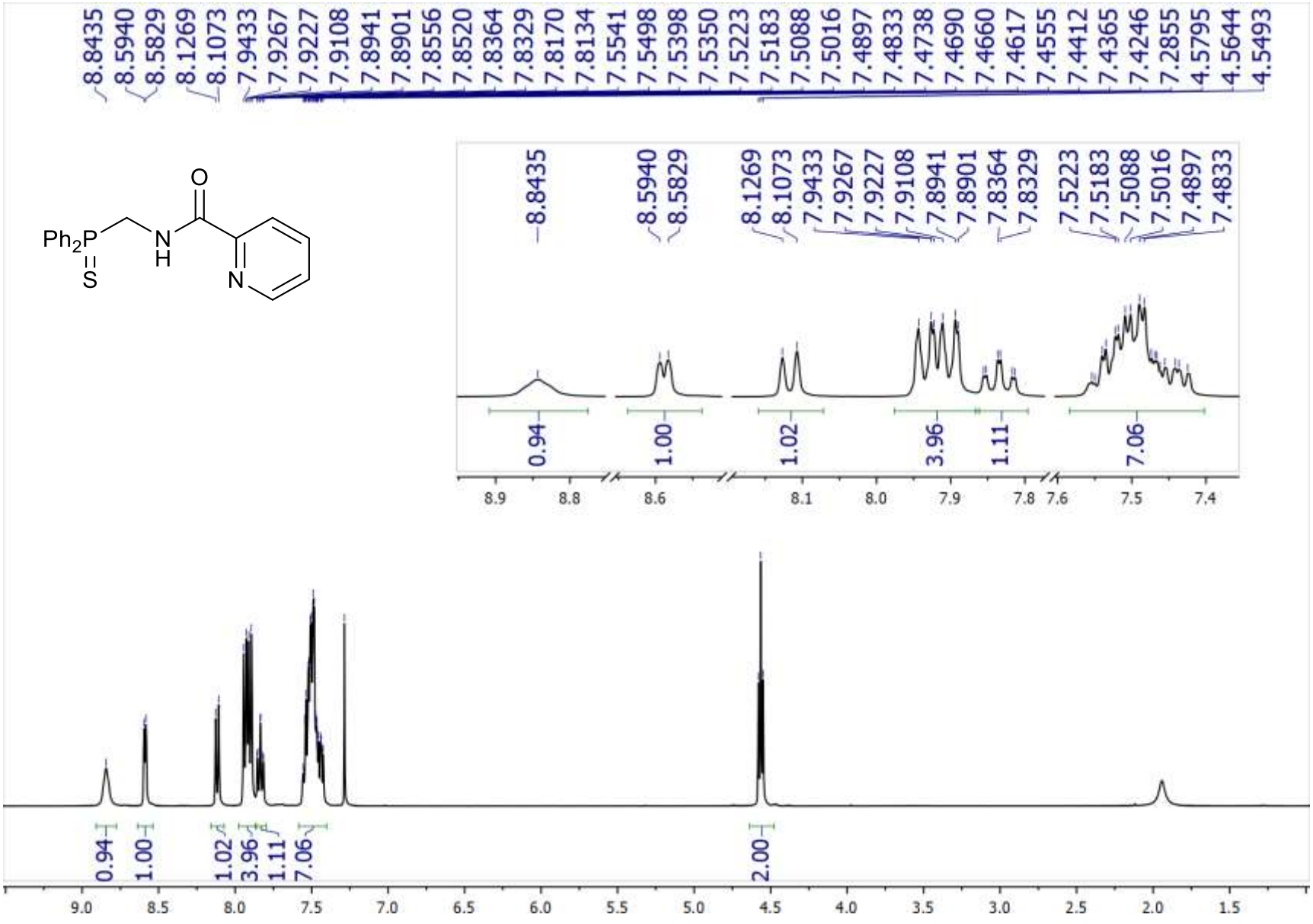

Figure S13. ^{1}H NMR spectrum of ligand **5** (400.13 MHz, $CDCl_3$)

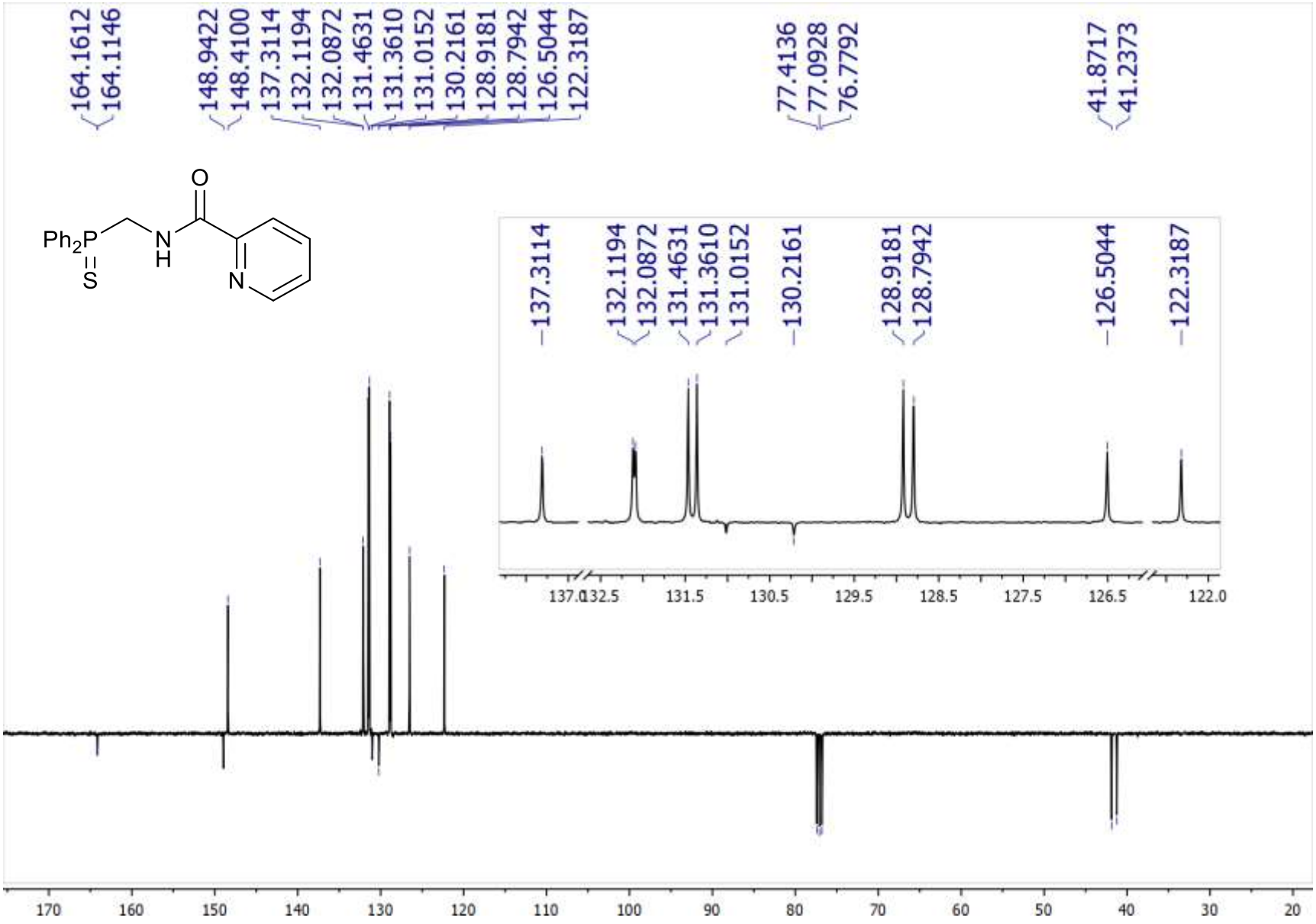

Figure S14. $^{13}C\{^{1}H\}$ NMR spectrum of ligand **5** (100.61 MHz, $CDCl_3$)

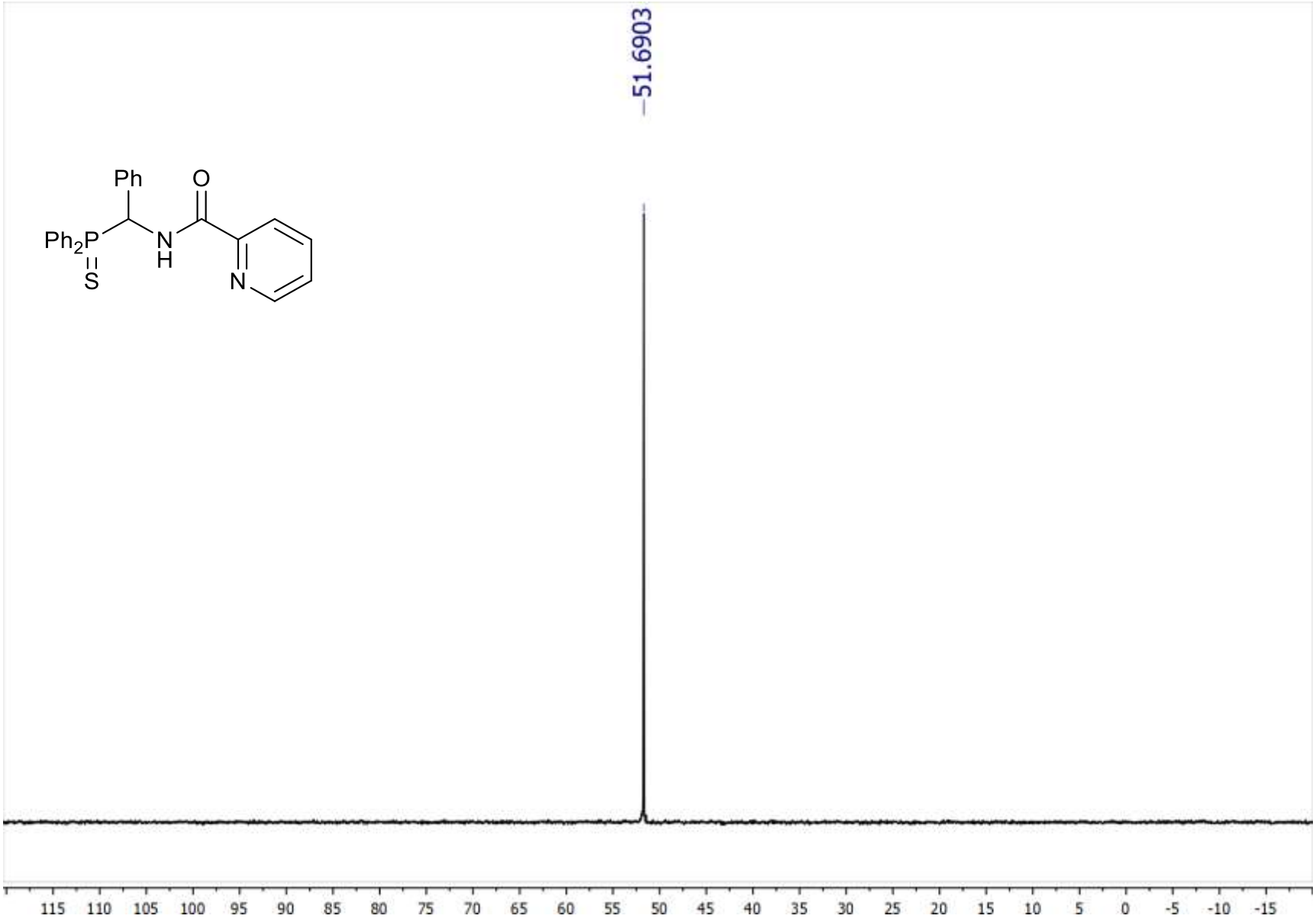

Figure S15. $^{31}P\{^{1}H\}$ NMR spectrum of ligand **6a** (161.98 MHz, $CDCl_3$)

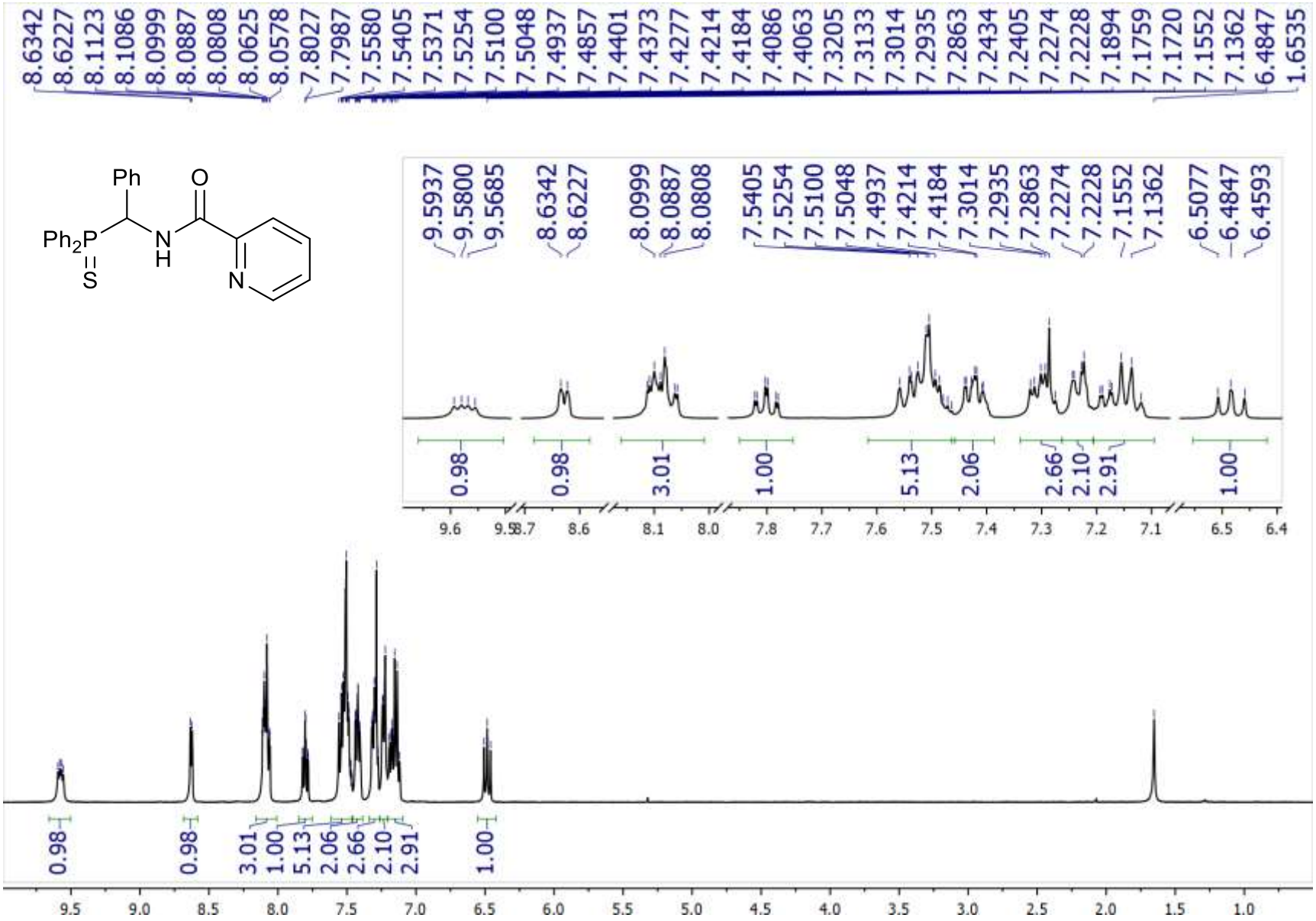

Figure S16. ^{1}H NMR spectrum of ligand **6a** (400.13 MHz, $CDCl_3$)

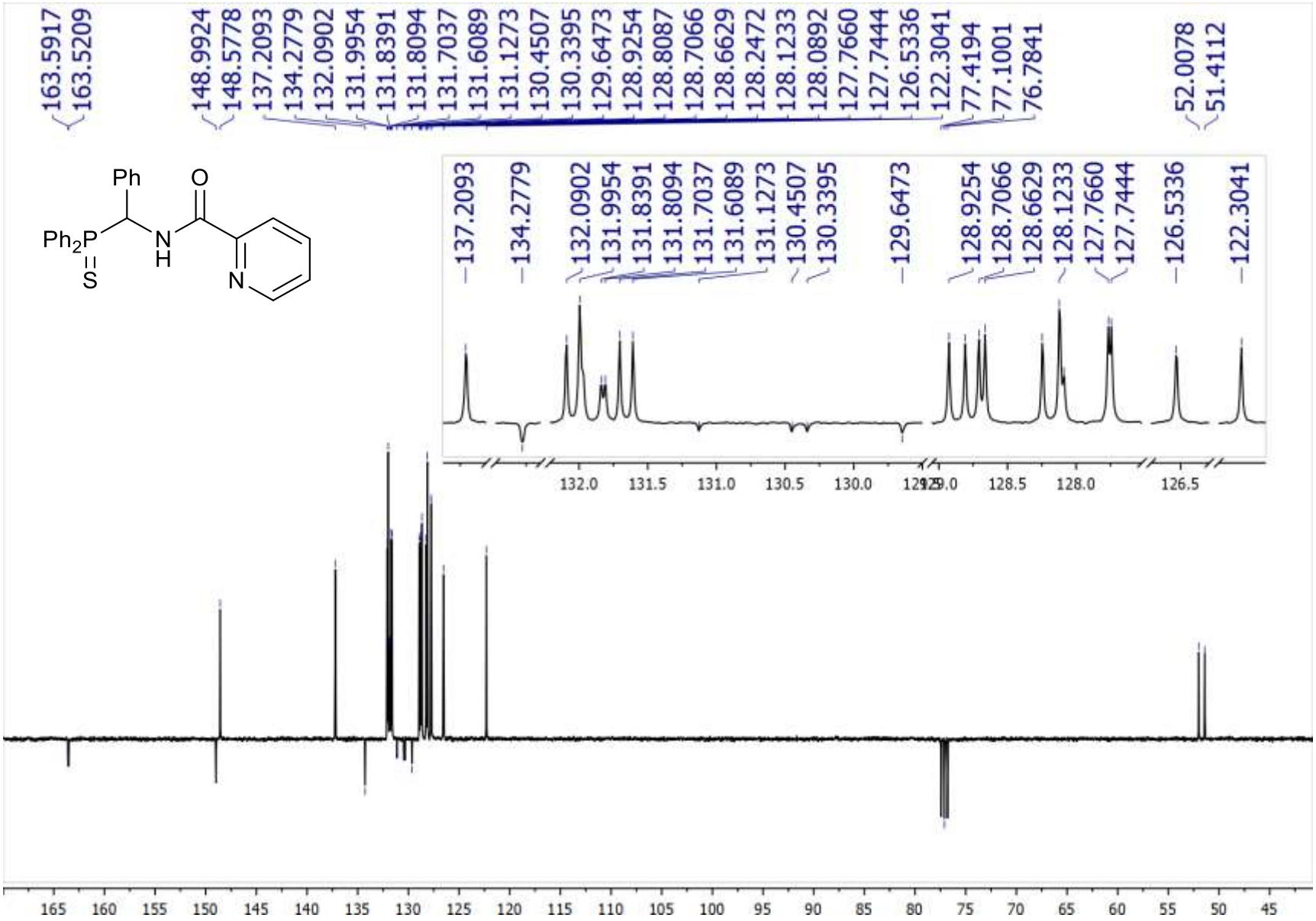

Figure S17. $^{13}C\{^{1}H\}$ NMR spectrum of ligand **6a** (100.61 MHz, $CDCl_3$)

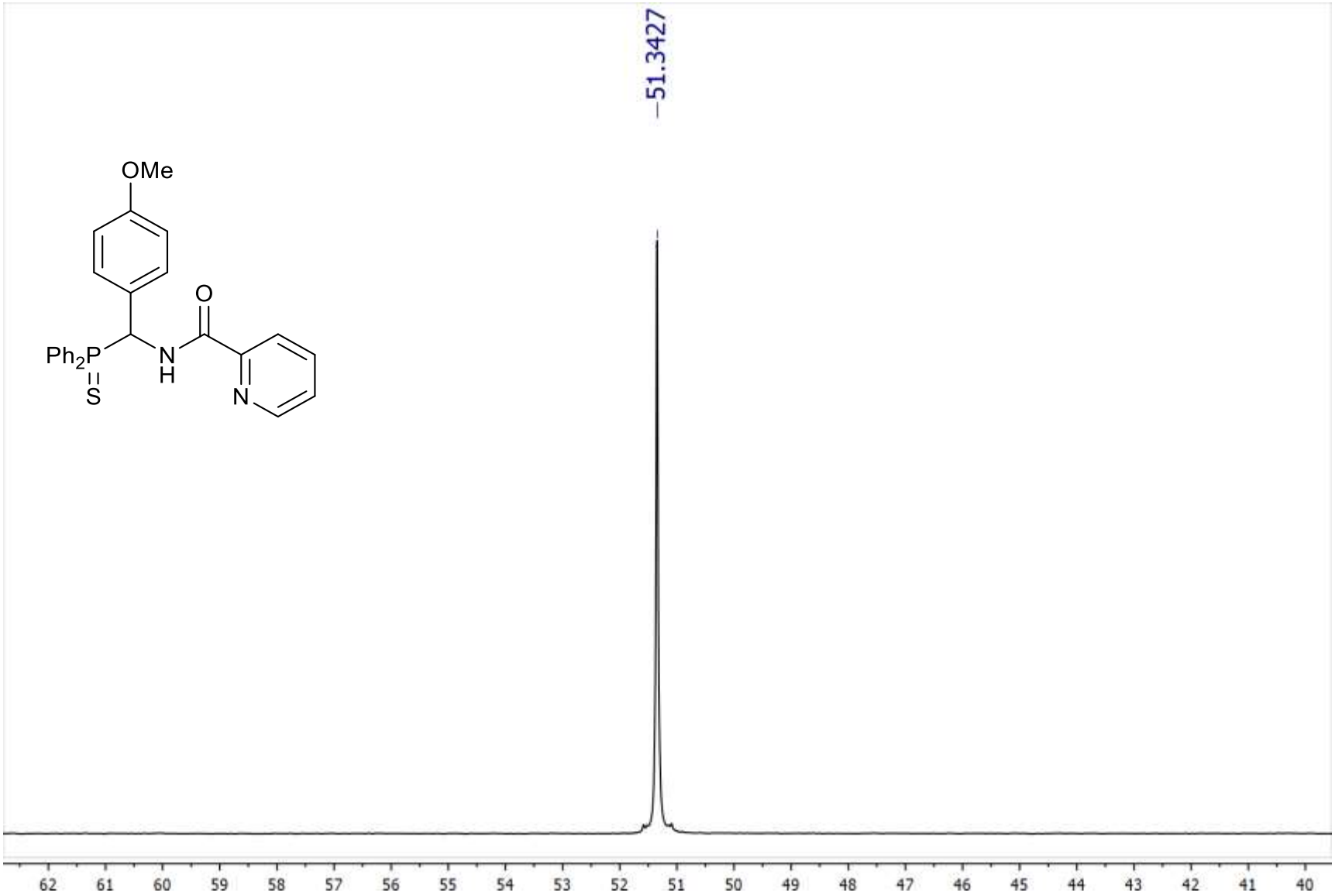

Figure S18. $^{31}P\{^{1}H\}$ NMR spectrum of ligand **6b** (161.98 MHz, $CDCl_3$)

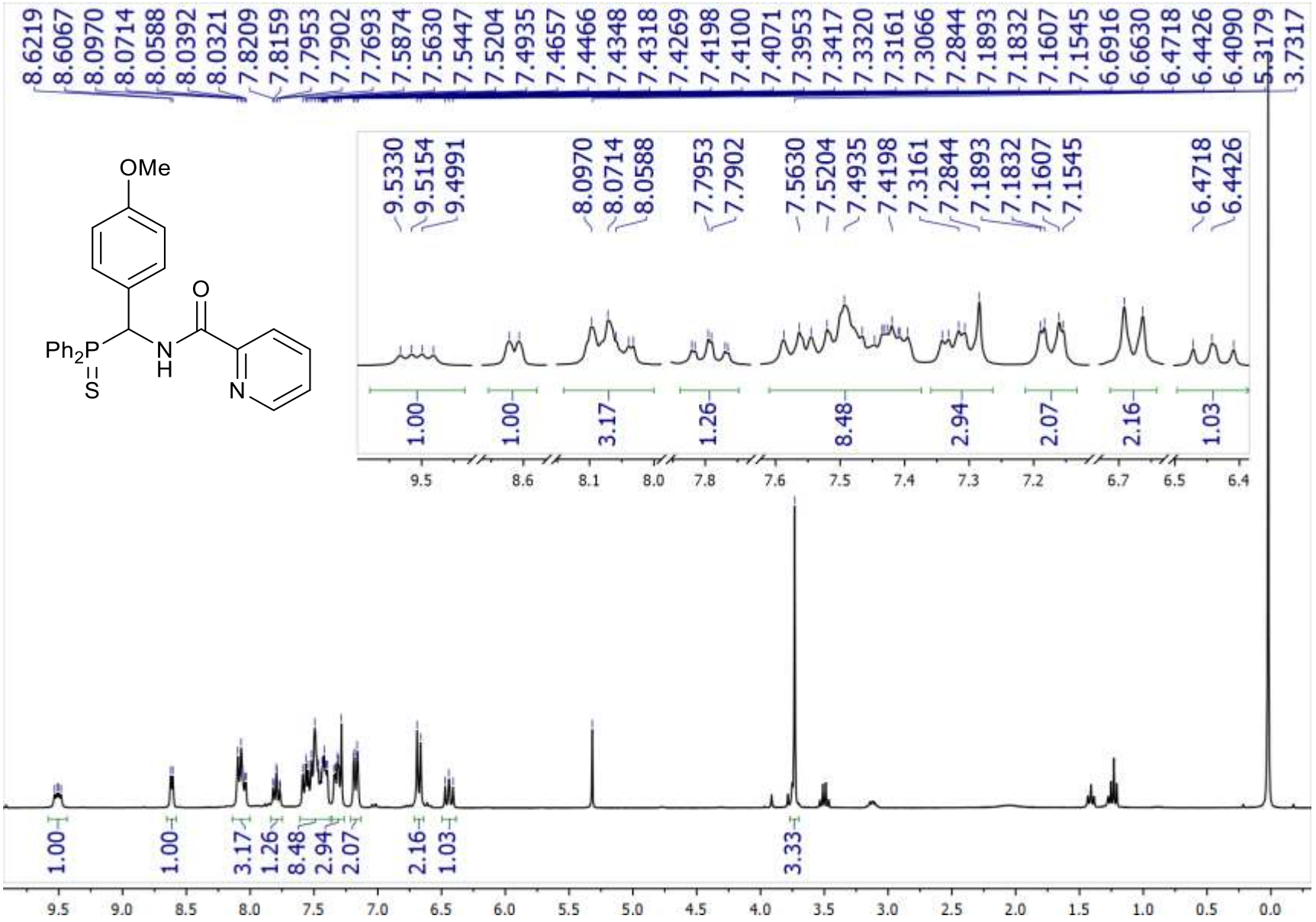

Figure S19. ^{1}H NMR spectrum of ligand **6b** (300.13 MHz, $CDCl_3$)

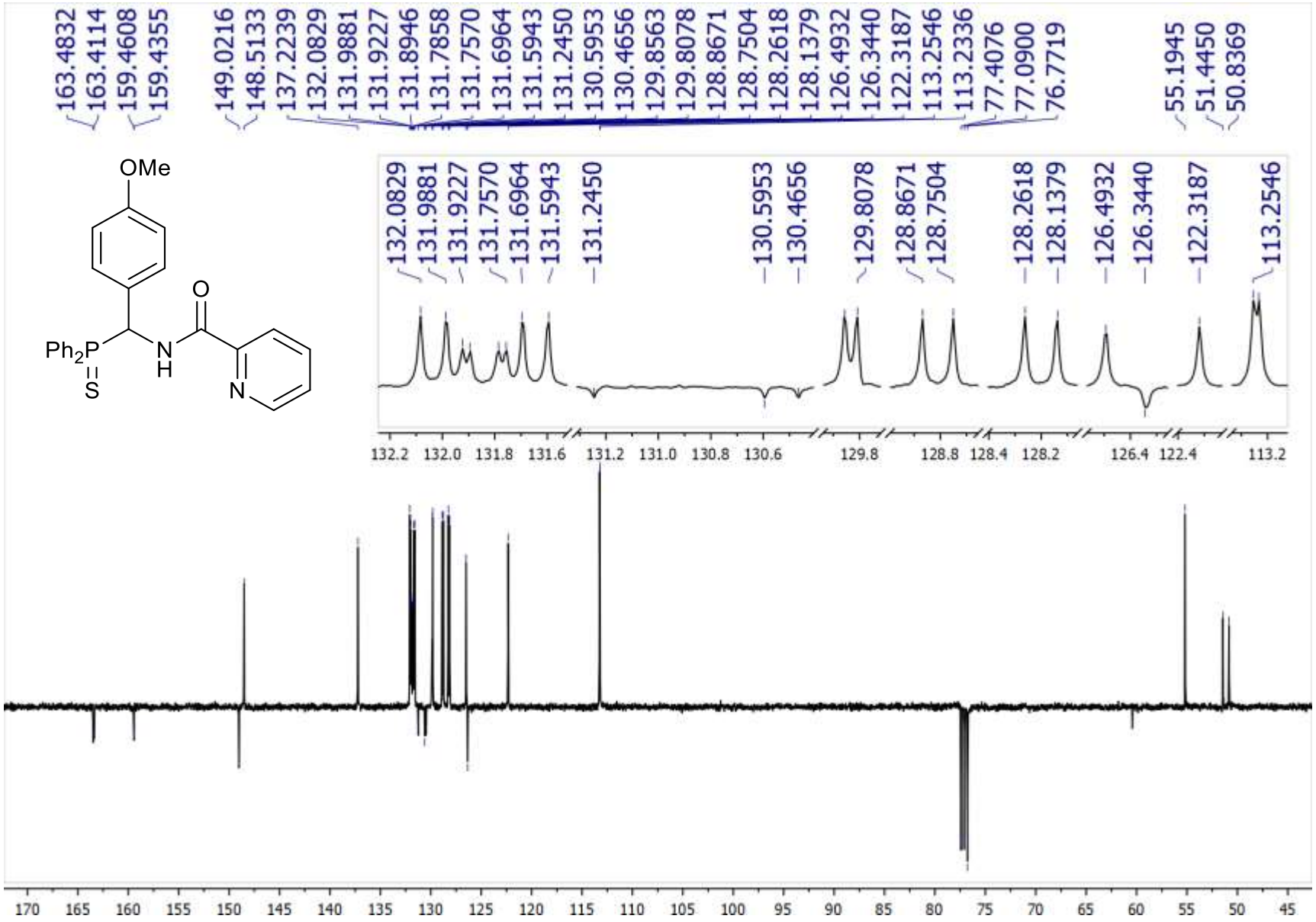

Figure S20. $^{13}C\{^{1}H\}$ NMR spectrum of ligand **6b** (100.61 MHz, $CDCl_3$)

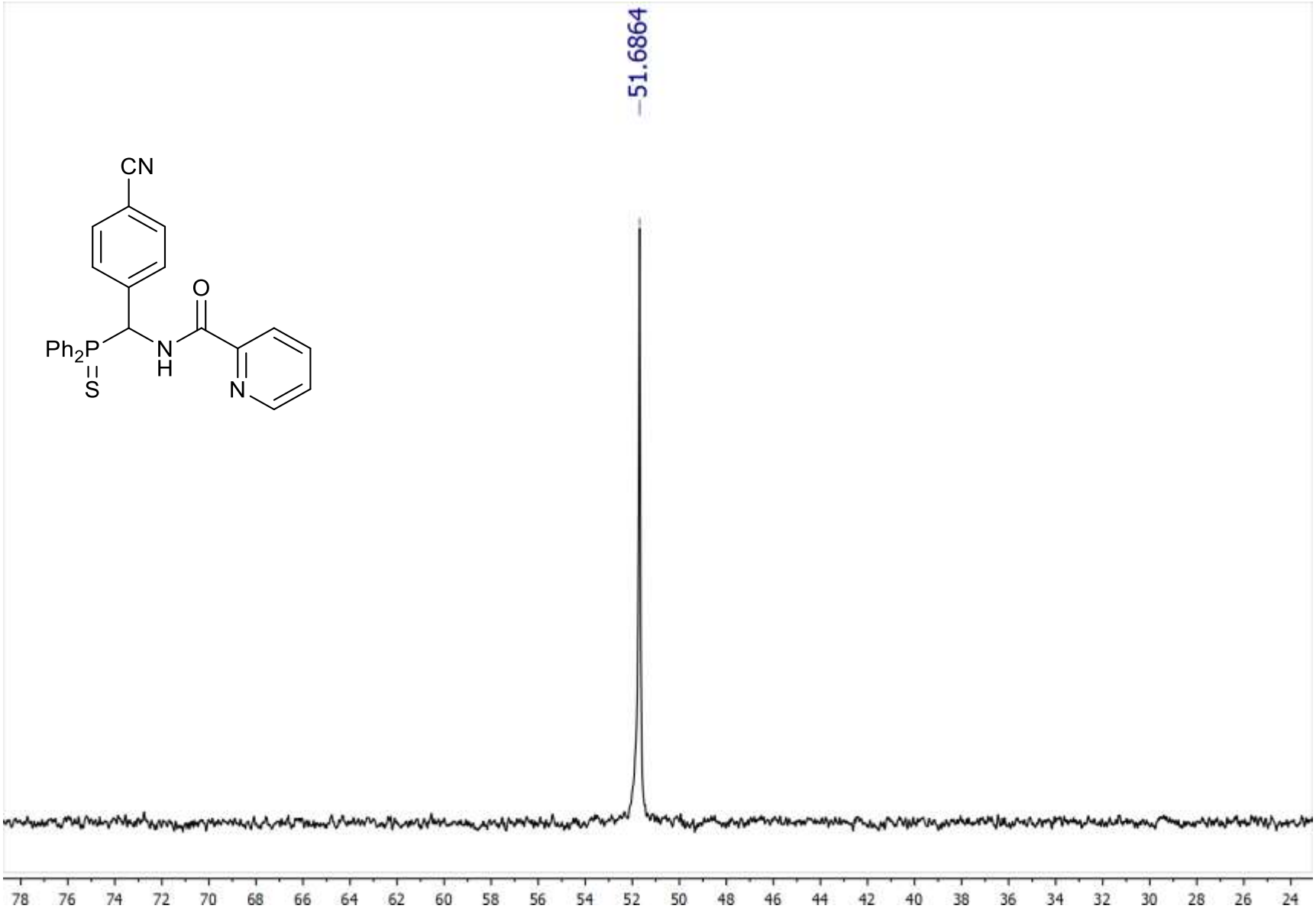

Figure S21. $^{31}P\{^{1}H\}$ NMR spectrum of ligand **6c** (121.49 MHz, $CDCl_3$)

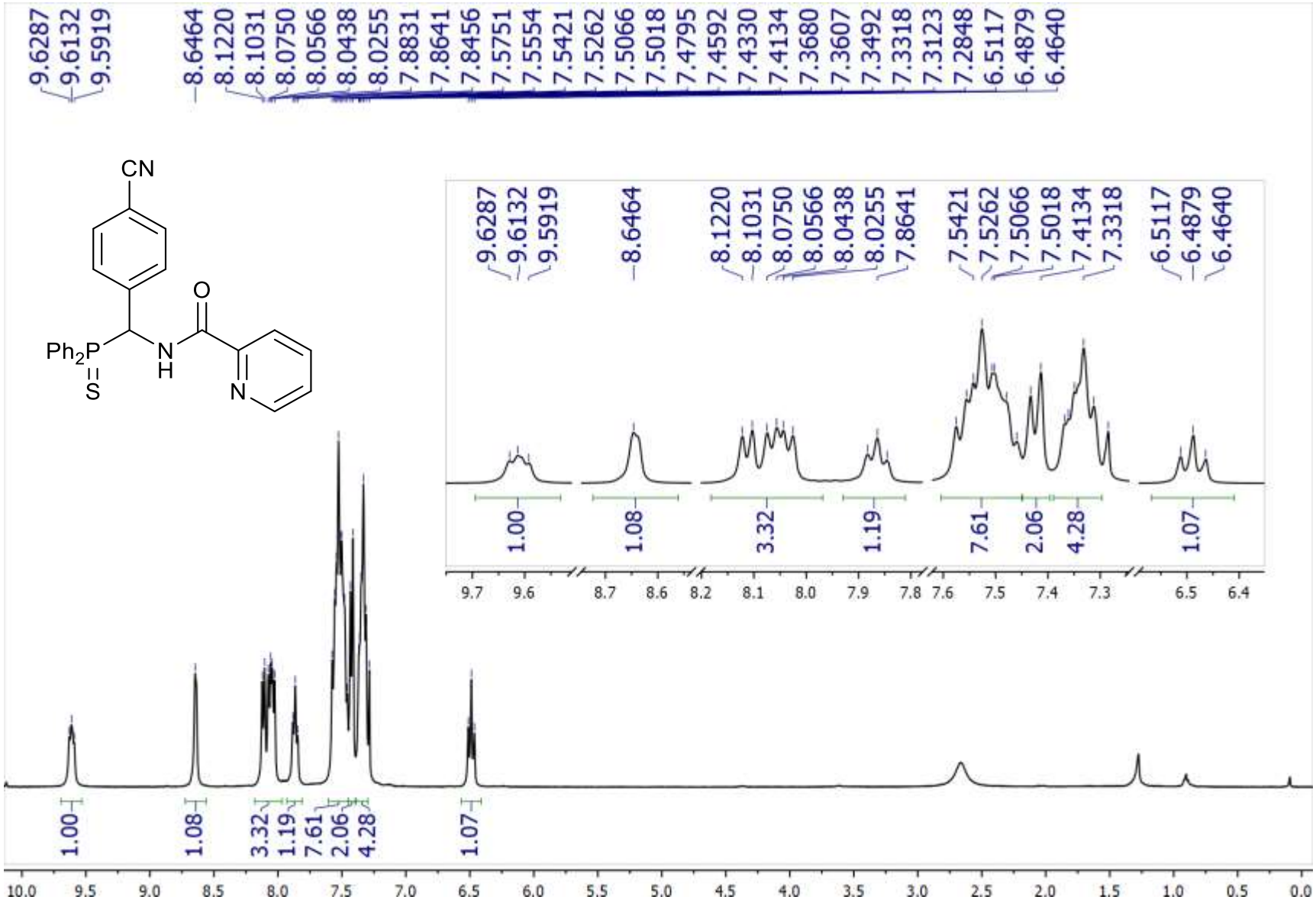

Figure S22. ^{1}H NMR spectrum of ligand **6c** (400.13 MHz, $CDCl_3$)

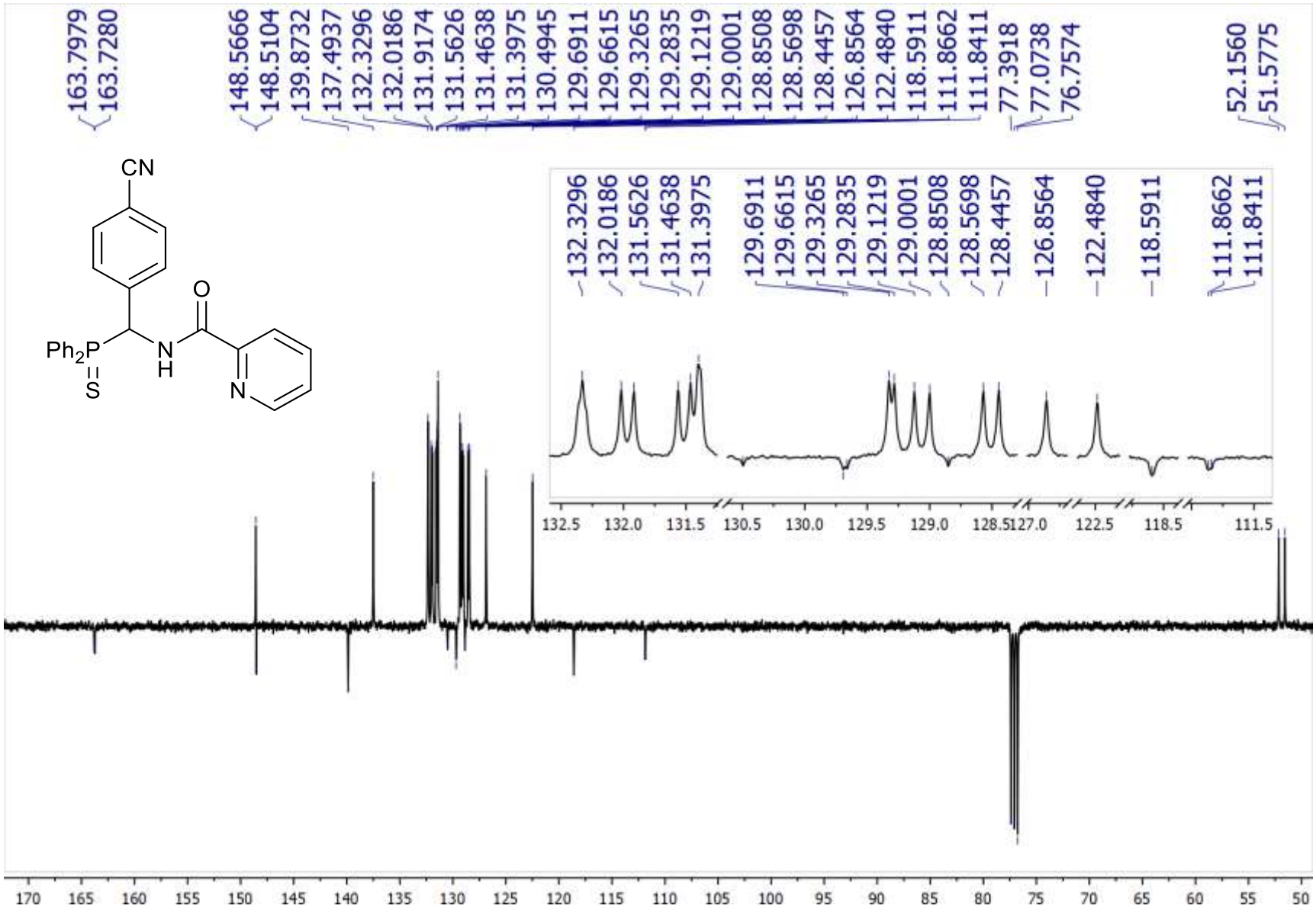

Figure S23. $^{13}C\{^{1}H\}$ NMR spectrum of ligand **6c** (100.61 MHz, $CDCl_3$)

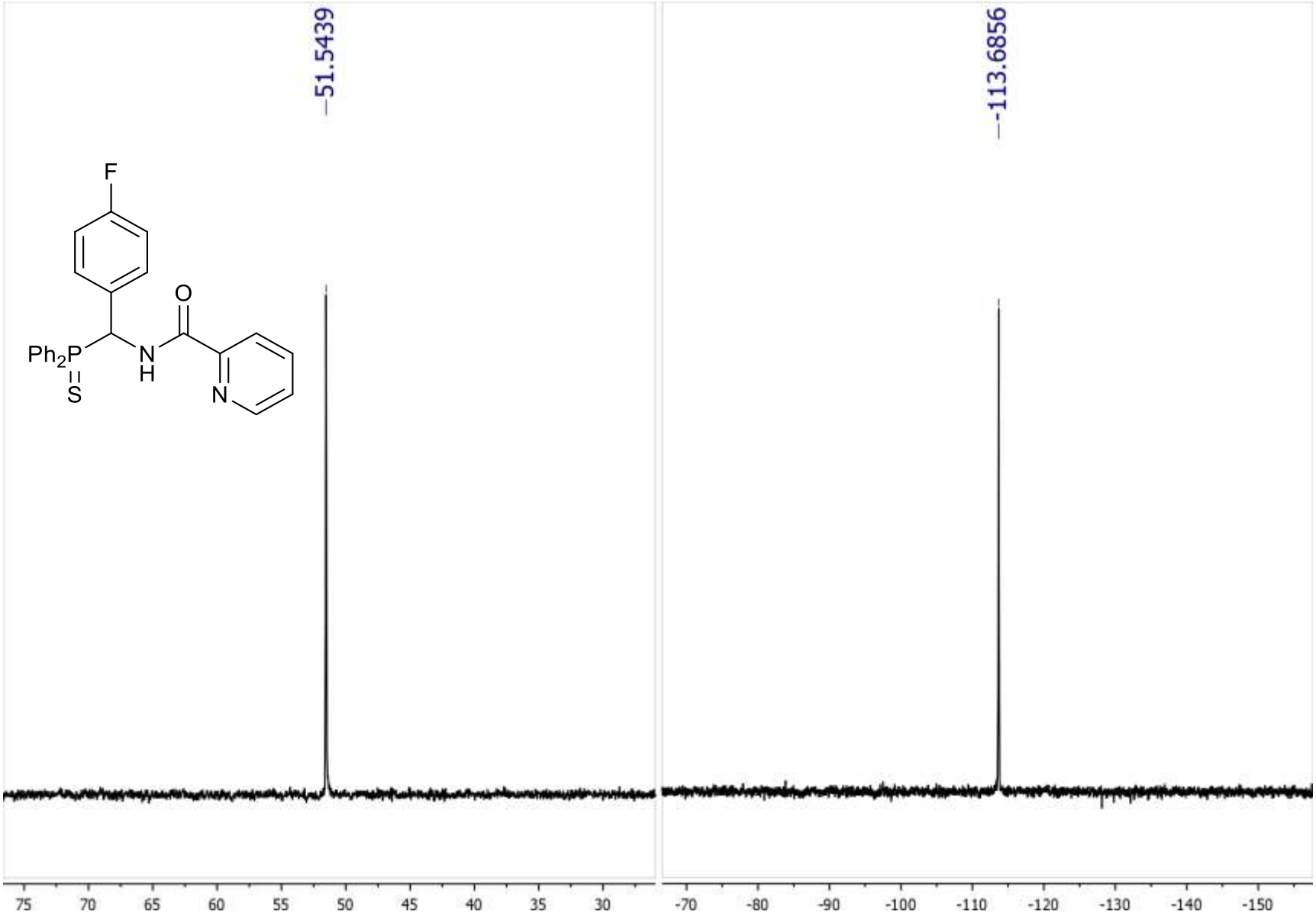

Figure S24. $^{31}P\{^{1}H\}$ (left) (161.98 MHz, $CDCl_3$) and $^{19}F\{^{1}H\}$ (right) (282.40 MHz, $CDCl_3$) NMR spectra of ligand **6d**

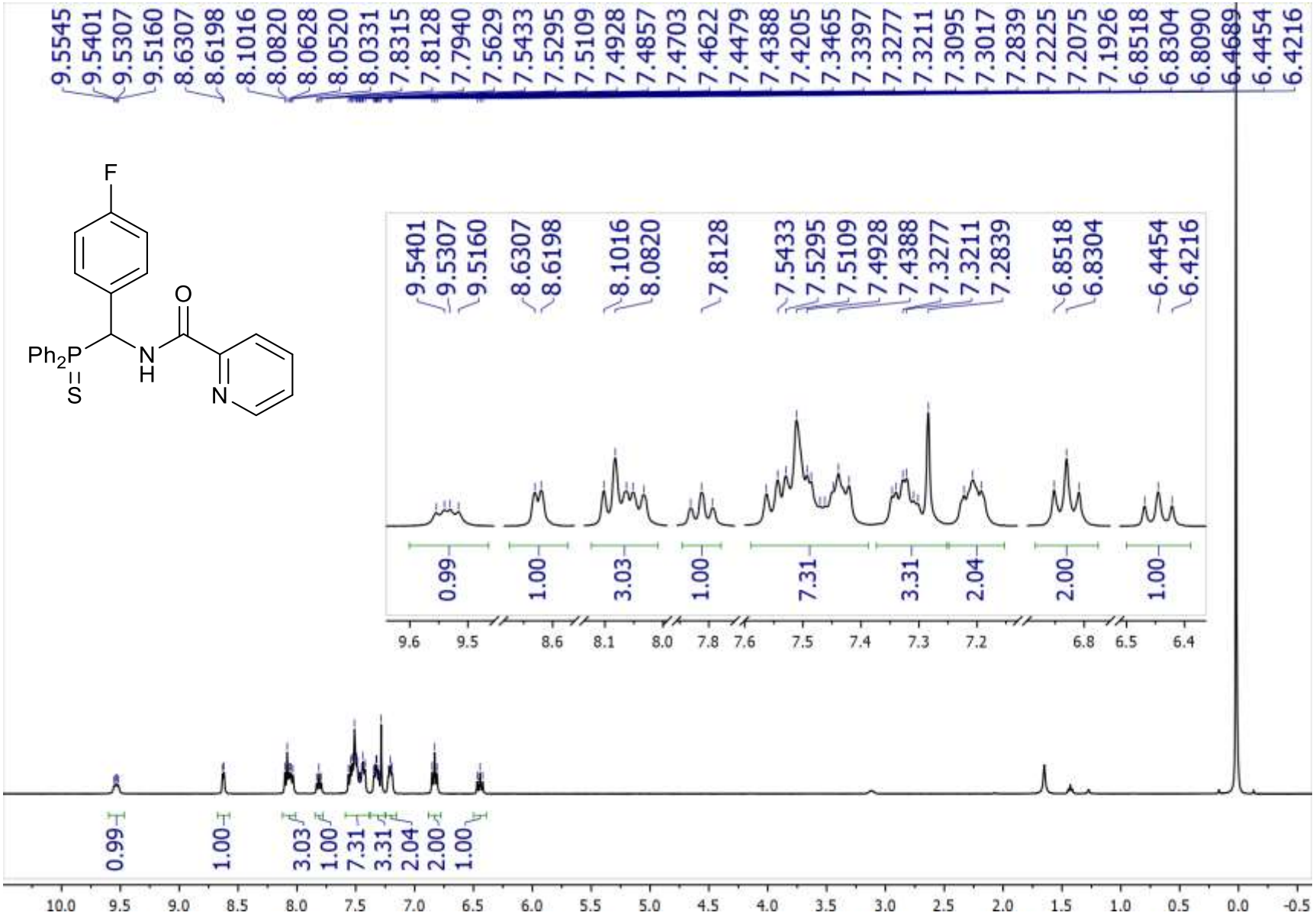

Figure S25. ^{1}H NMR spectrum of ligand **6d** (400.13 MHz, $CDCl_3$)

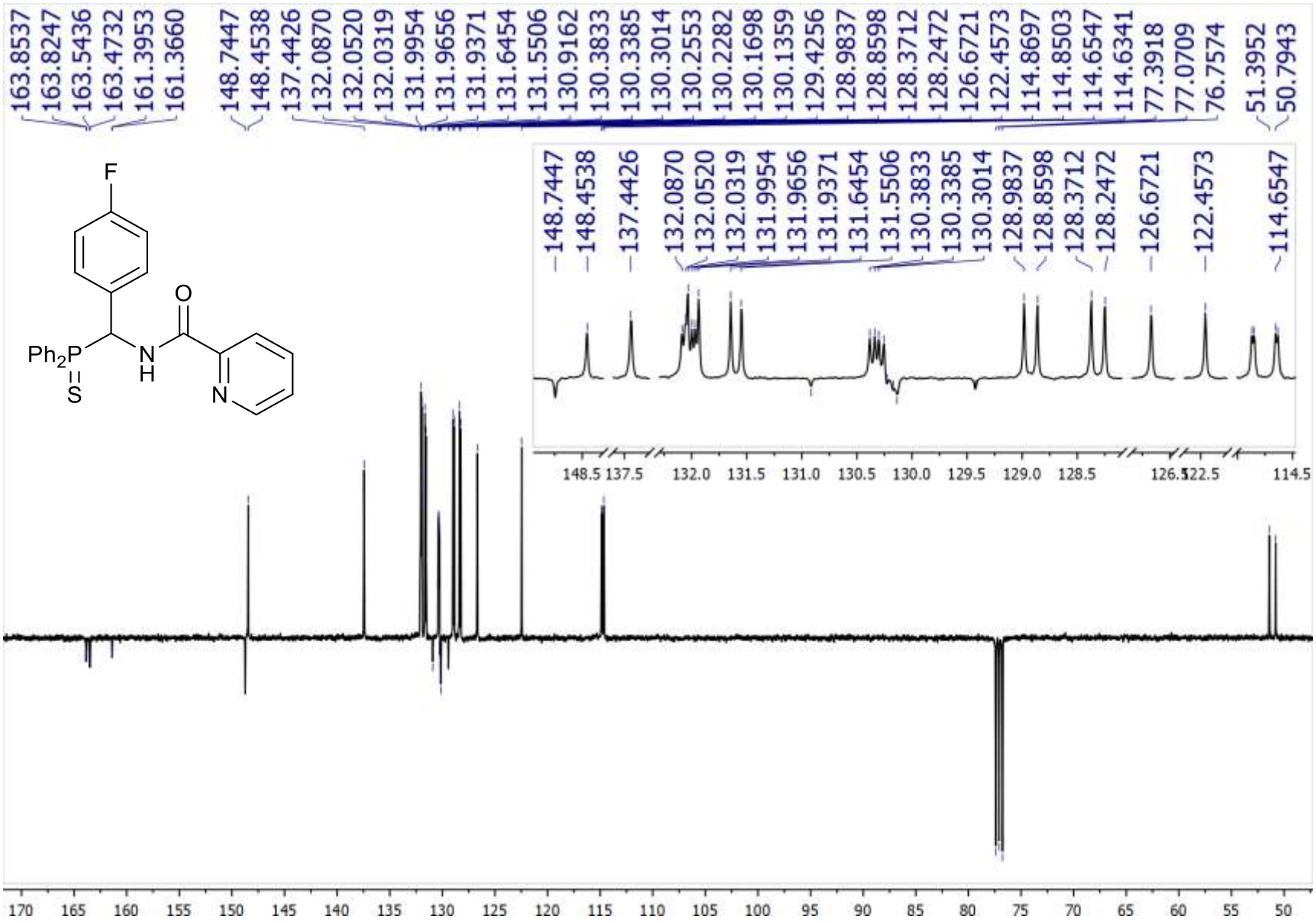

Figure S26. $^{13}C\{^{1}H\}$ NMR spectrum of ligand **6d** (100.61 MHz, $CDCl_3$)

Figure S27. $^{31}P\{^{1}H\}$ NMR spectrum of complex **7** (161.98 MHz, $CDCl_3$)

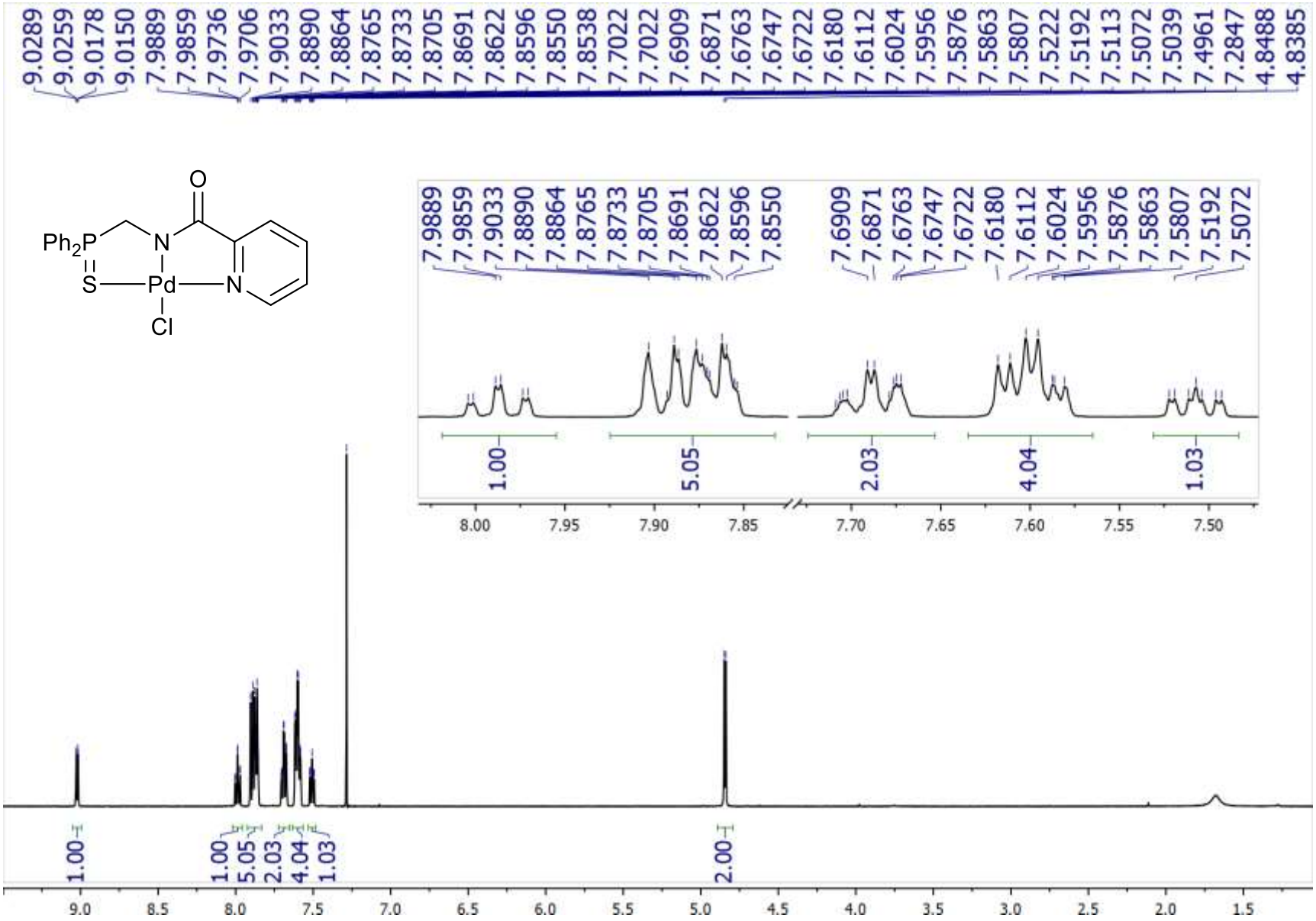

Figure S28. ^{1}H NMR spectrum of complex **7** (500.13 MHz, $CDCl_3$)

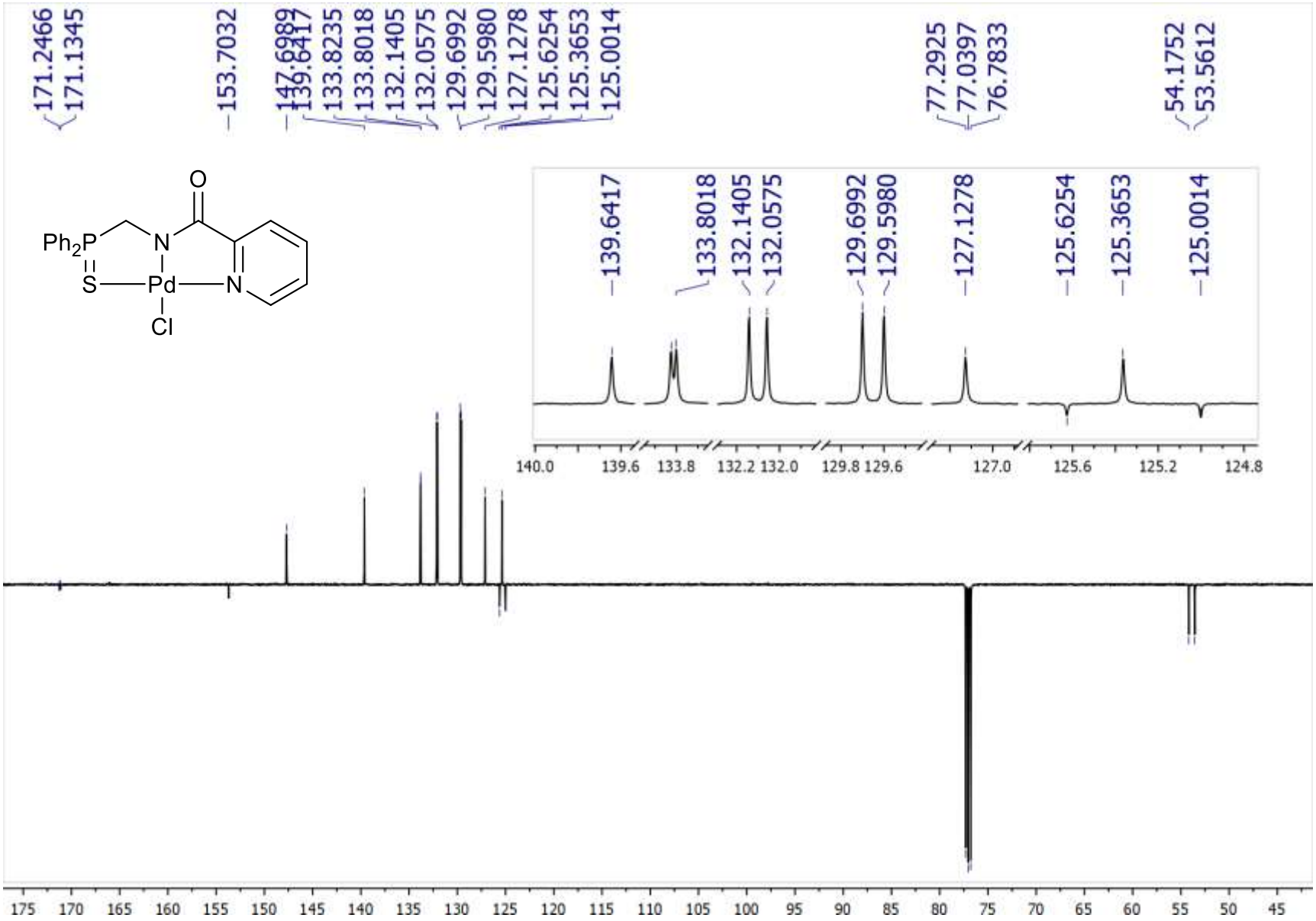

Figure S29. $^{13}C\{^{1}H\}$ NMR spectrum of complex **7** (125.76 MHz, $CDCl_3$)

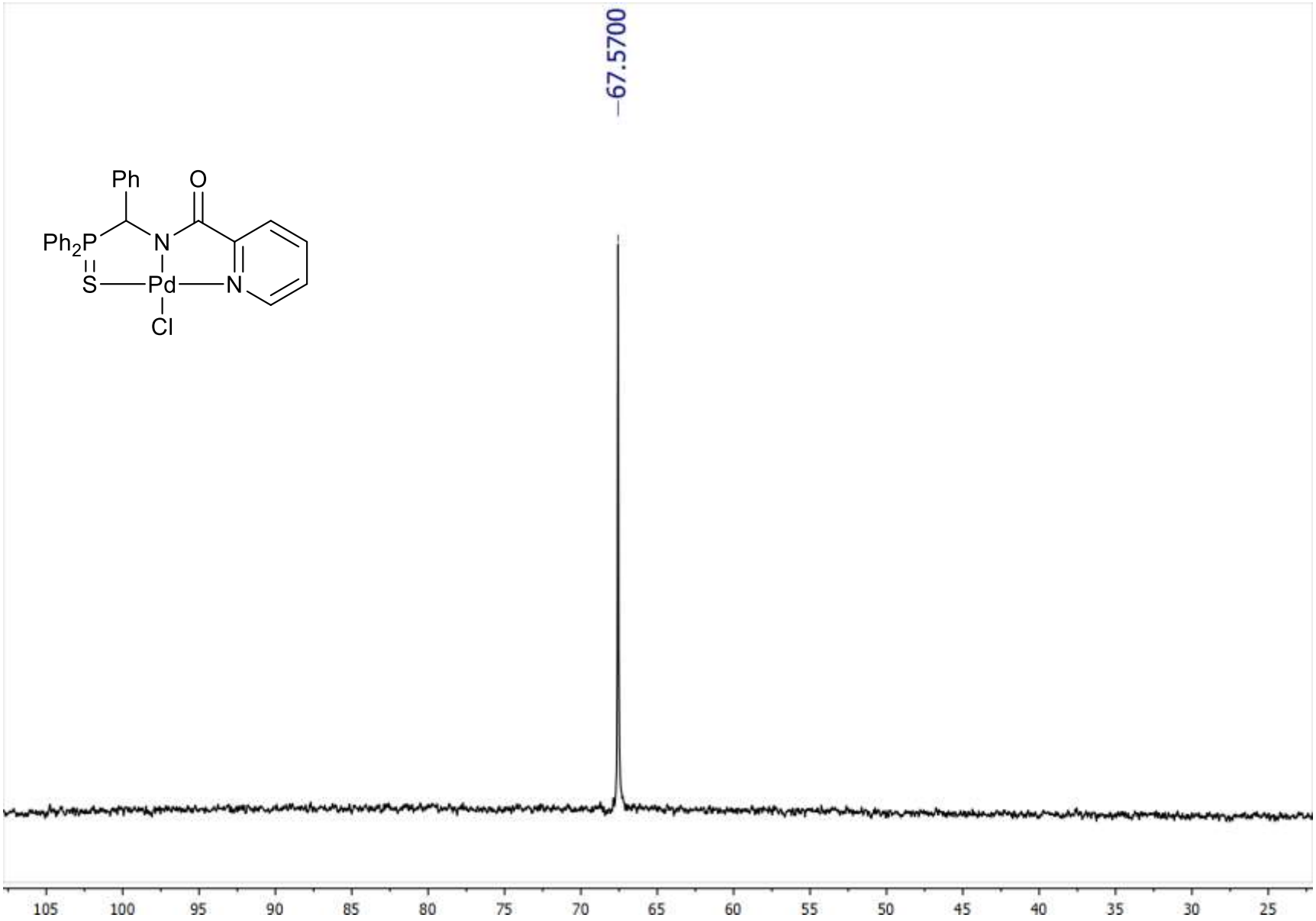

Figure S30. $^{31}P\{^{1}H\}$ NMR spectrum of complex **8a** (121.49 MHz, $CDCl_3$)

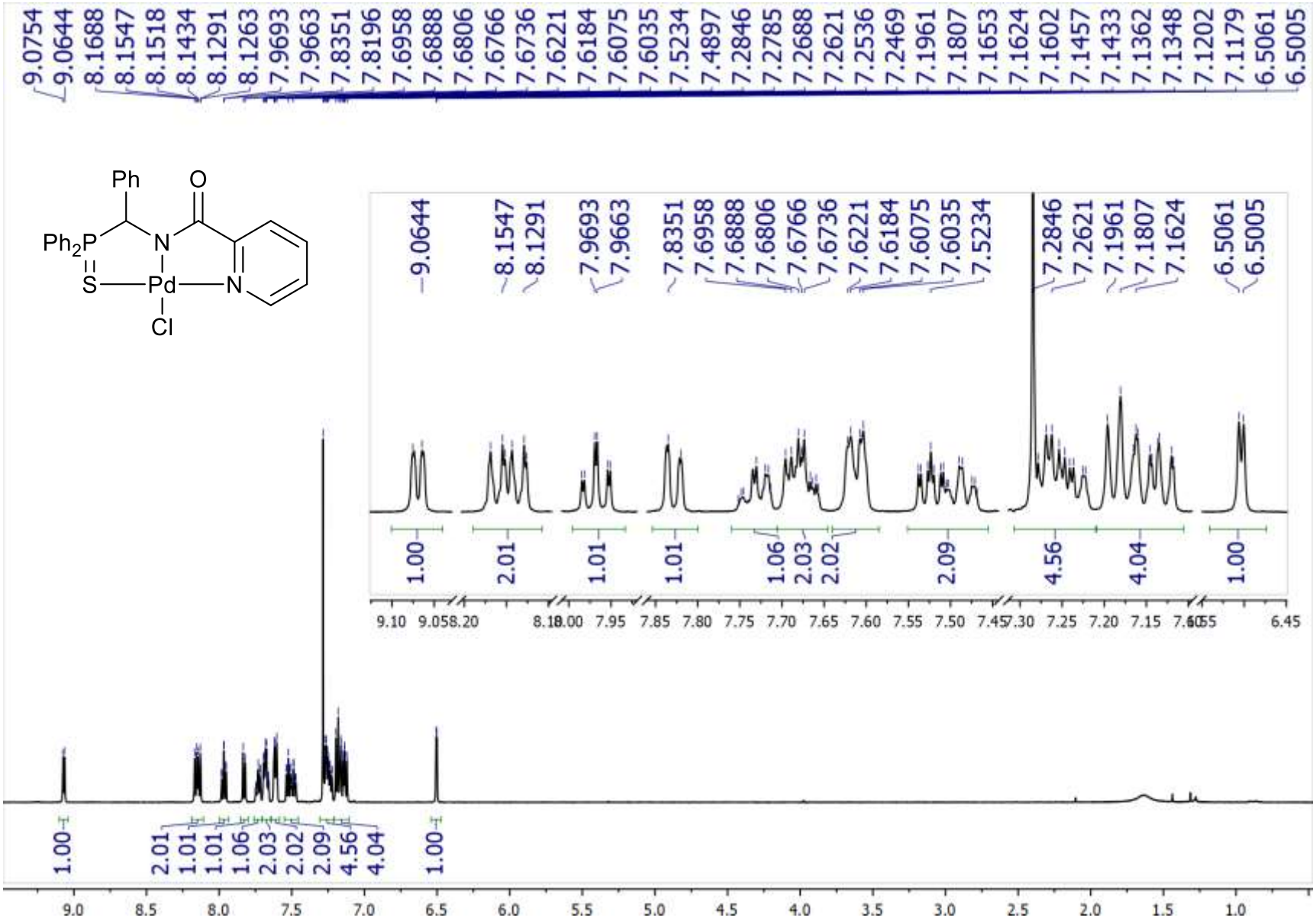

Figure S31. ^{1}H NMR spectrum of complex **8a** (500.13 MHz, $CDCl_3$)

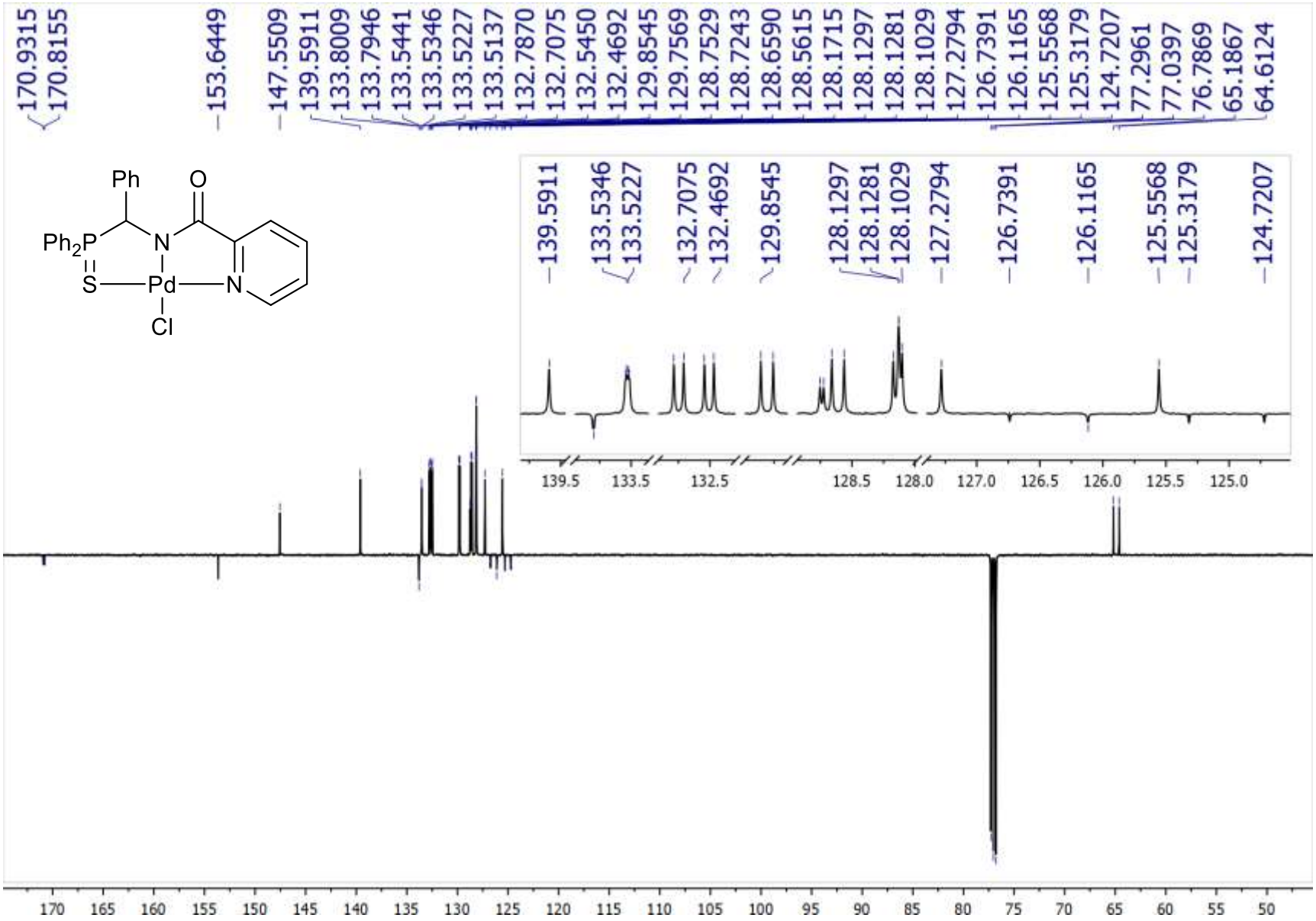

Figure S32. $^{13}C\{^{1}H\}$ NMR spectrum of complex **8a** (125.76 MHz, $CDCl_3$)

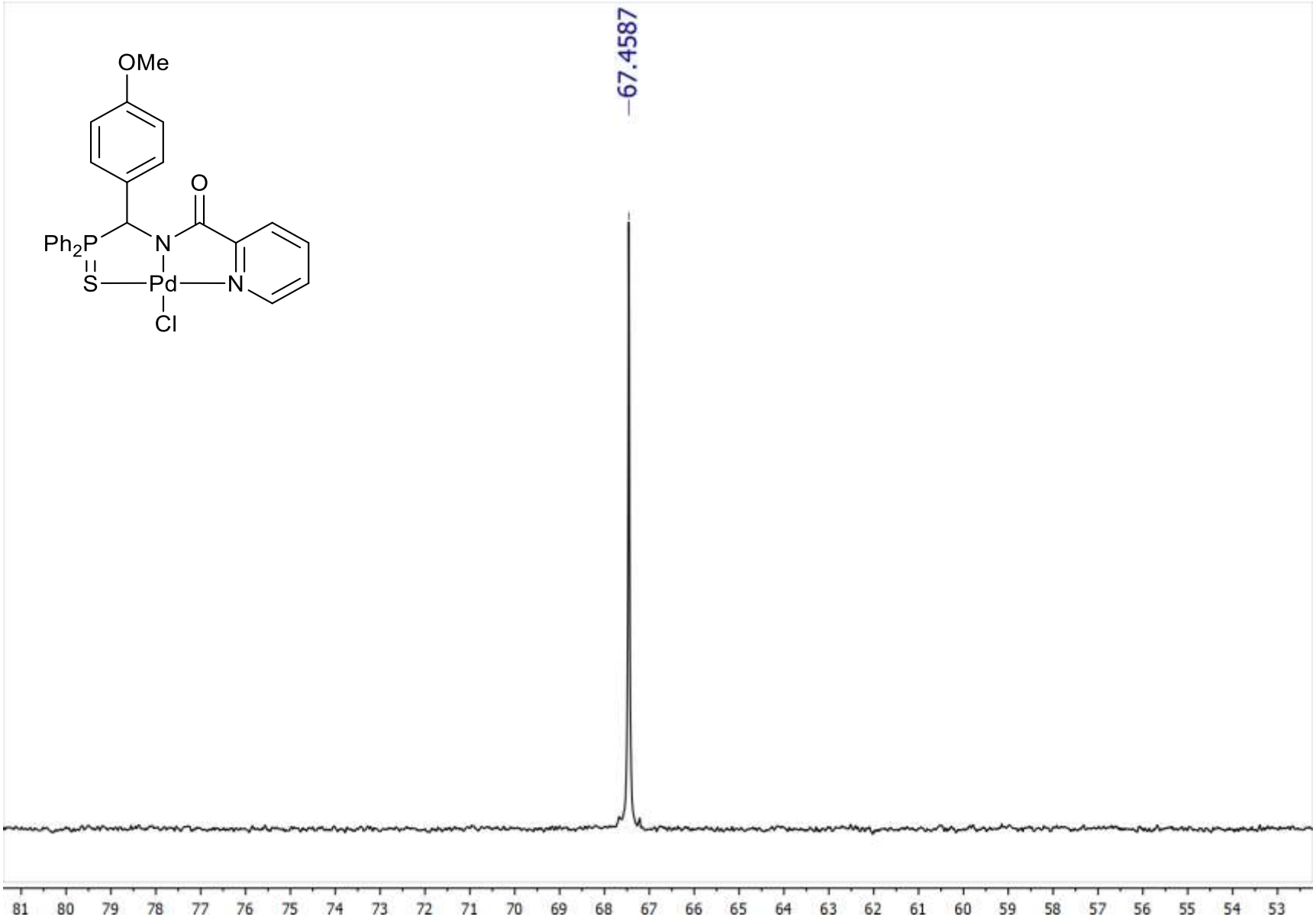

Figure S33. $^{31}P\{^{1}H\}$ NMR spectrum of complex **8b** (161.98 MHz, $(CD_3)_2SO$)

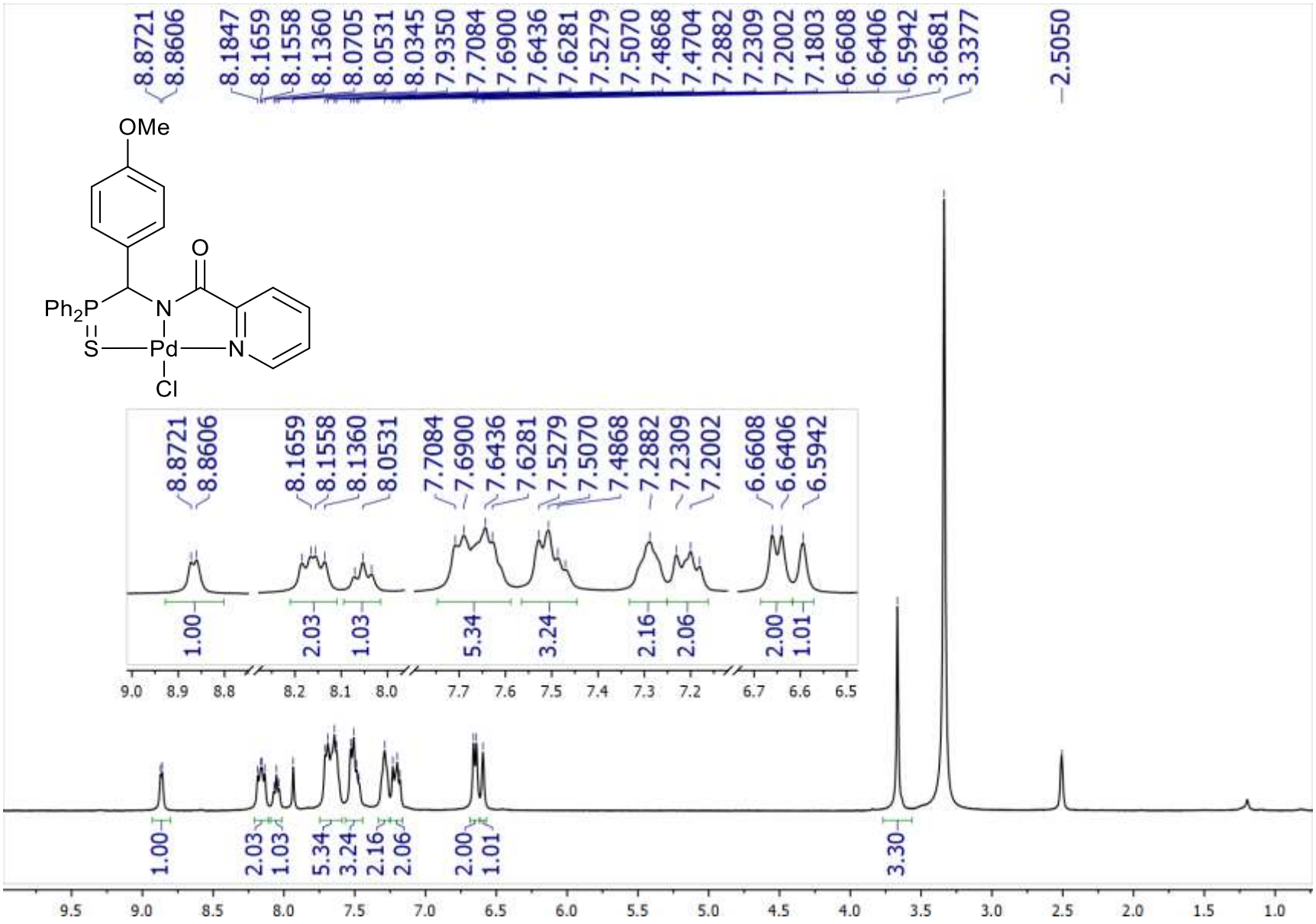

Figure S34. ^{1}H NMR spectrum of complex **8b** (400.13 MHz, $CDCl_3$/$(CD_3)_2SO$)

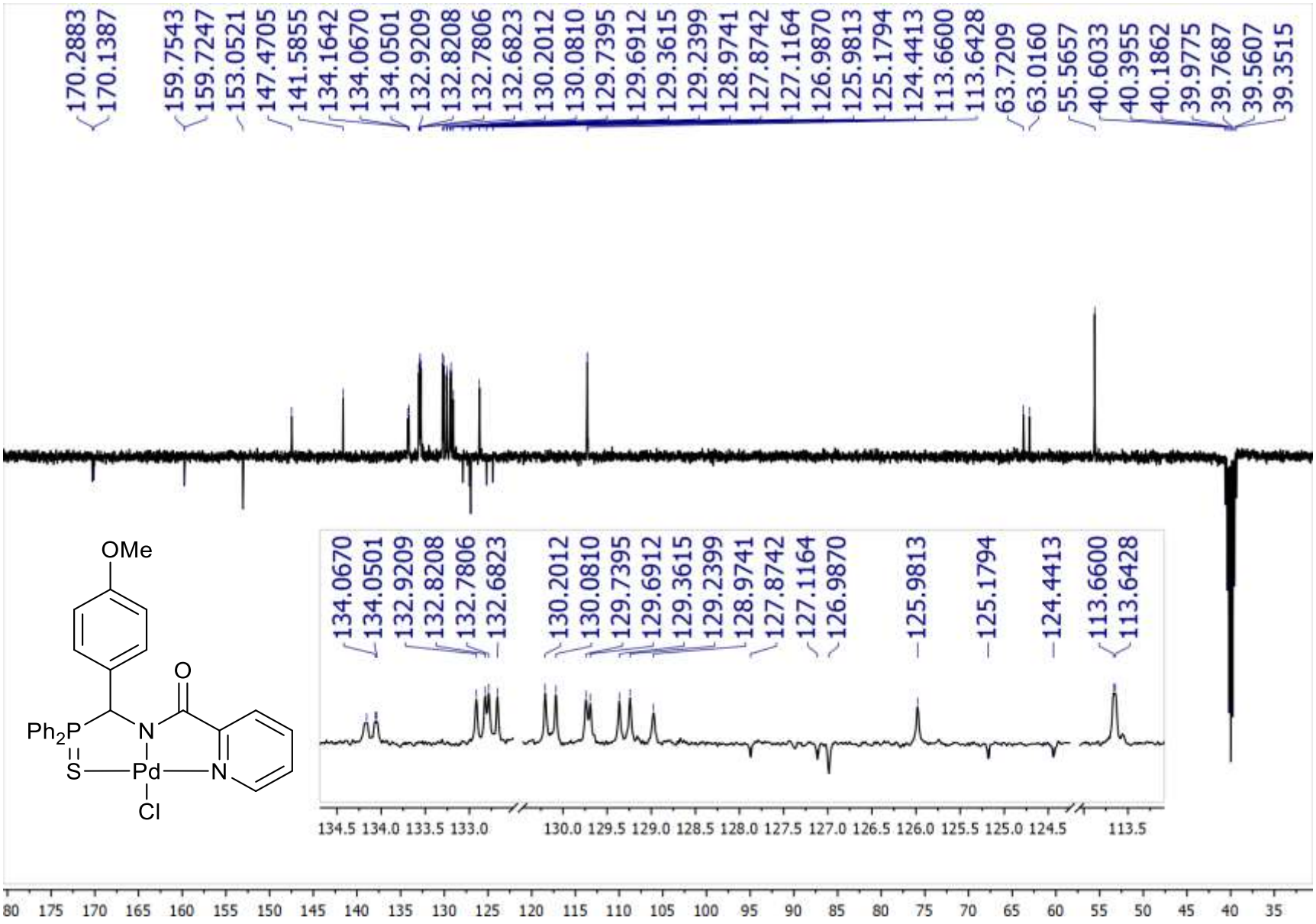

Figure S35. $^{13}C\{^{1}H\}$ NMR spectrum of complex **8b** (100.61 MHz, $(CD_3)_2SO$)

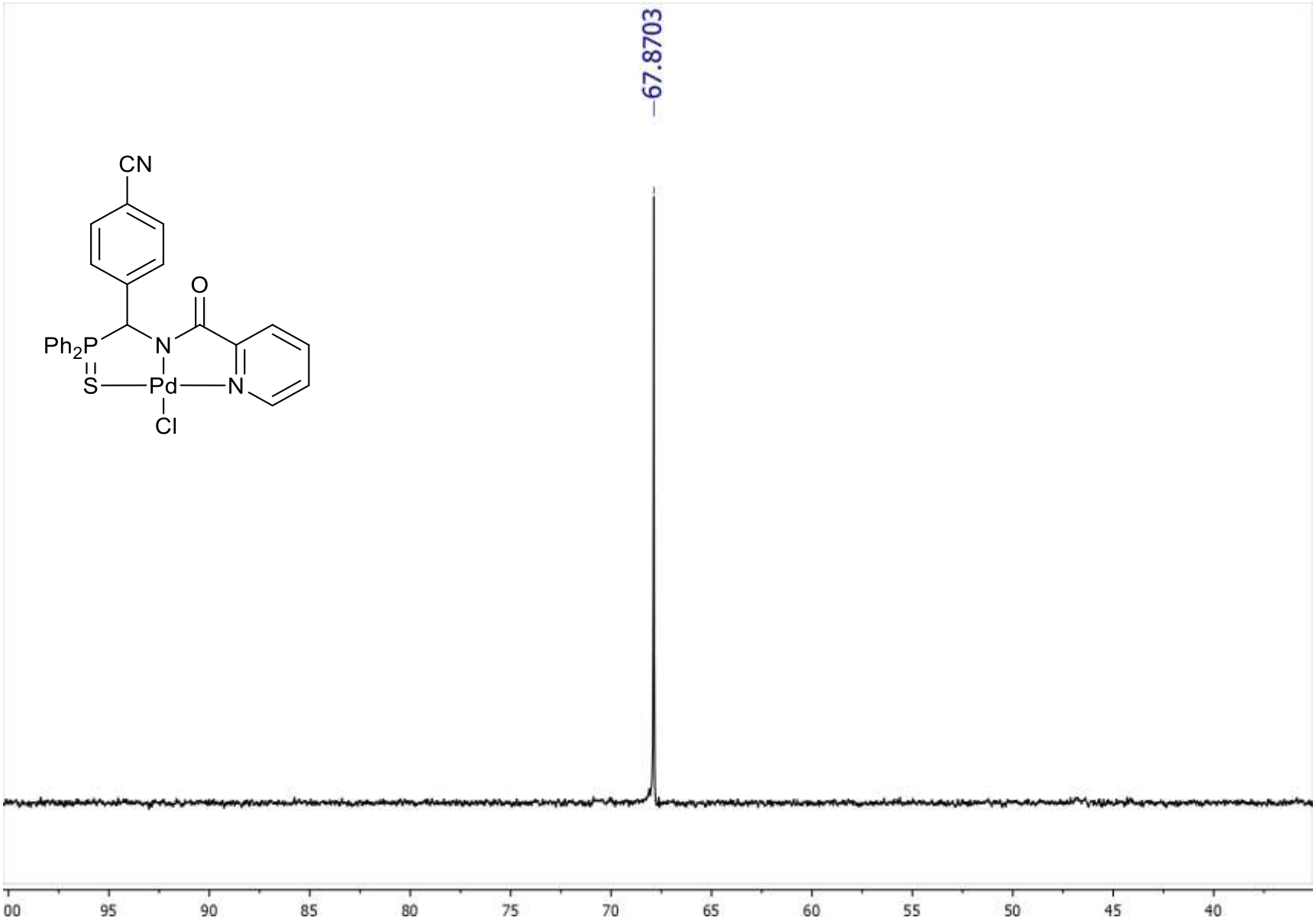

Figure S36. $^{31}P\{^{1}H\}$ NMR spectrum of complex **8c** (161.98 MHz, $CDCl_3$)

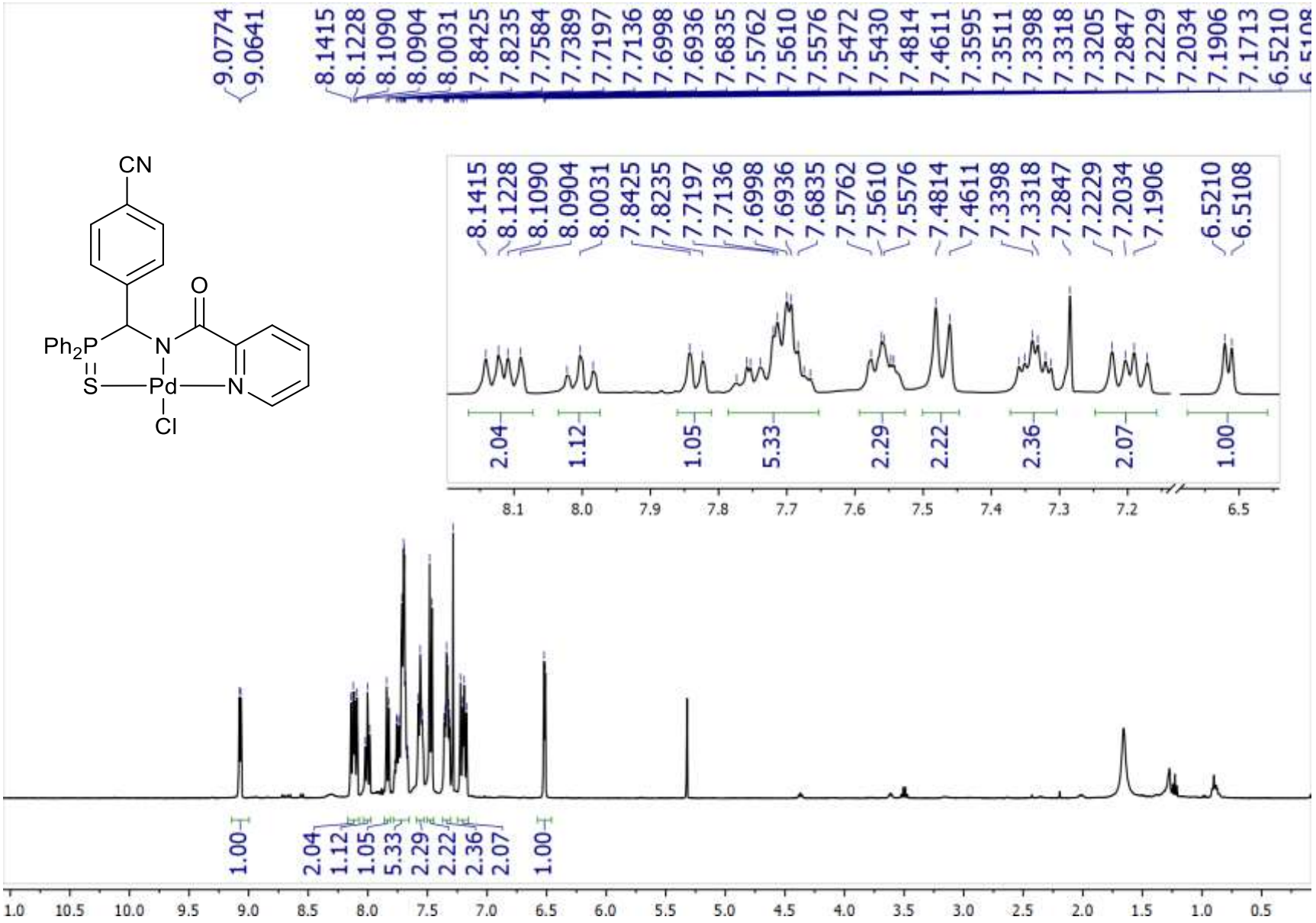

Figure S37. ^{1}H NMR spectrum of complex **8c** (400.13 MHz, $CDCl_3$)

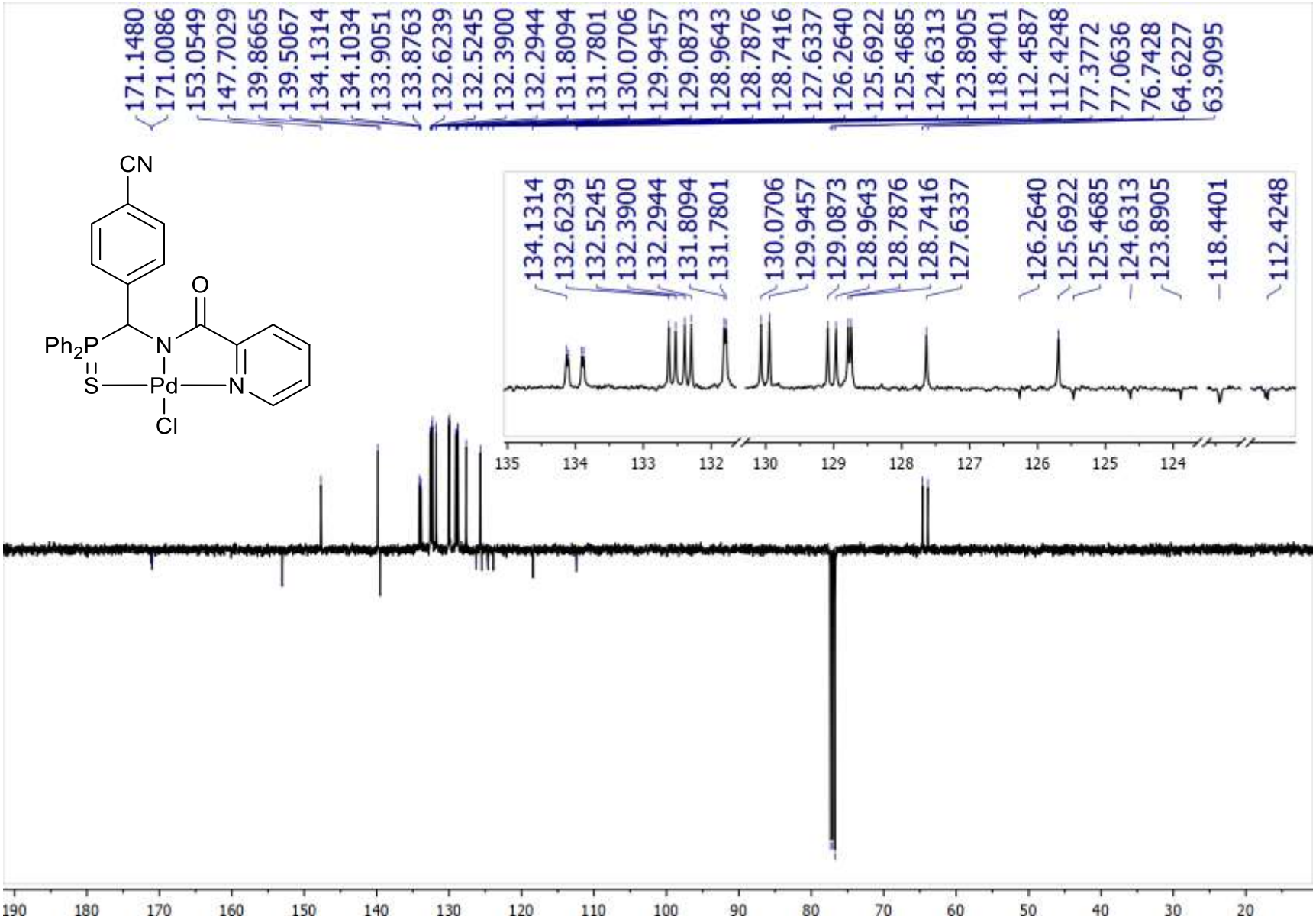

Figure S38. $^{13}C\{^{1}H\}$ NMR spectrum of complex **8c** (100.61 MHz, $CDCl_3$)

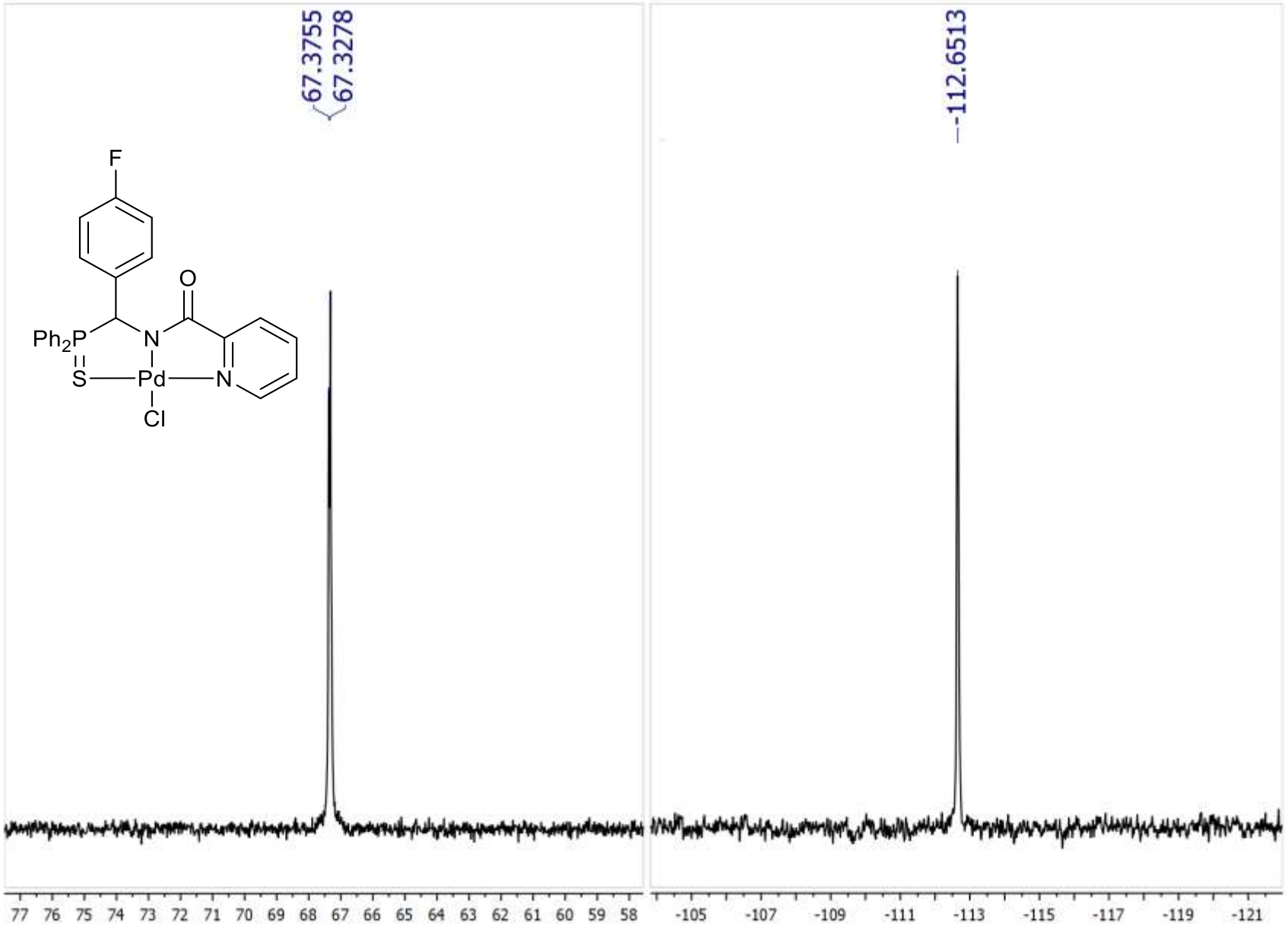

Figure S39. $^{31}P\{^{1}H\}$ (left) (121.49 MHz, $CDCl_3$) and $^{19}F\{^{1}H\}$ (right) (282.40 MHz, $CDCl_3$) NMR spectra of complex **8d**

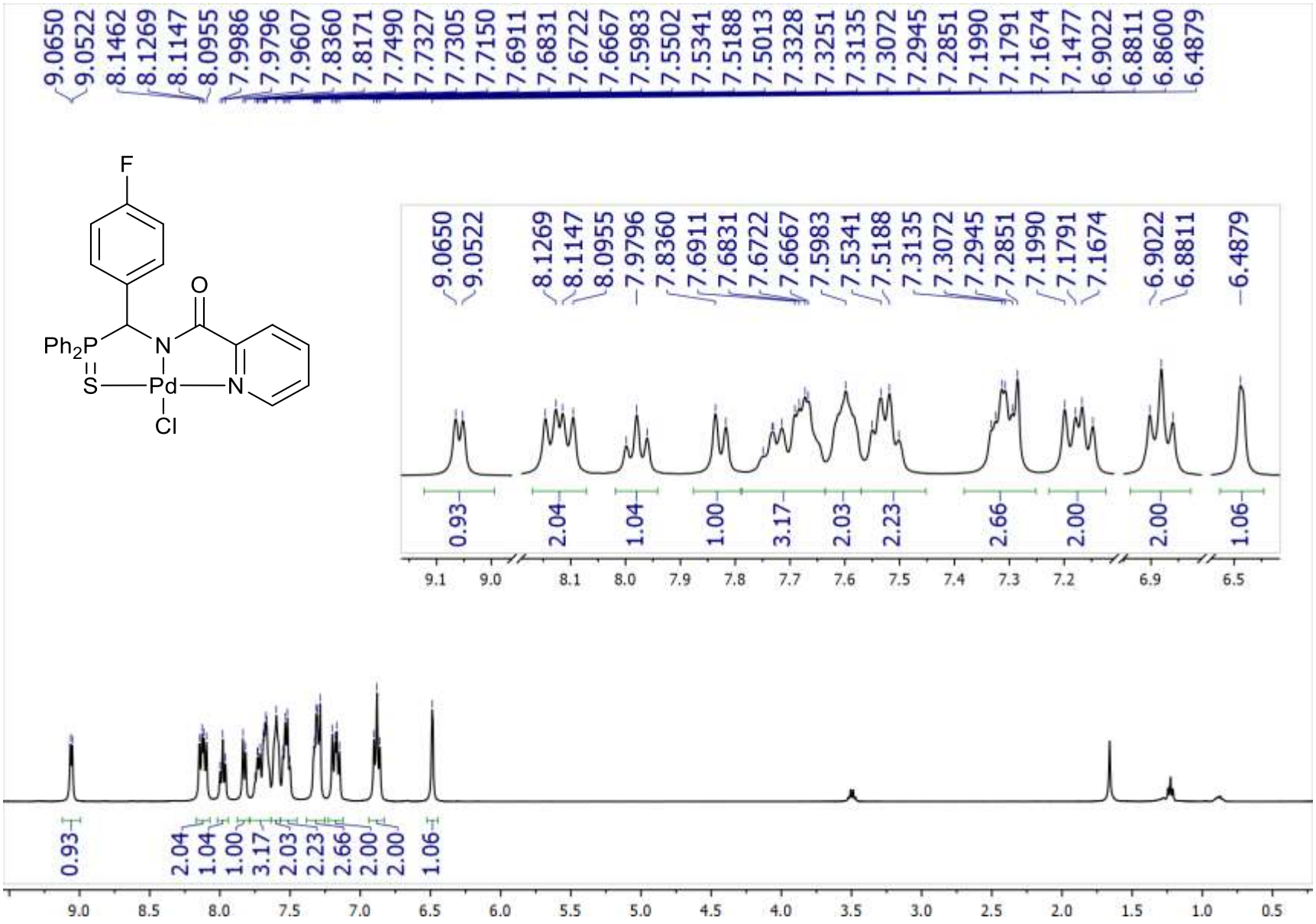

Figure S40. ^{1}H NMR spectrum of complex **8d** (400.13 MHz, $CDCl_3$)

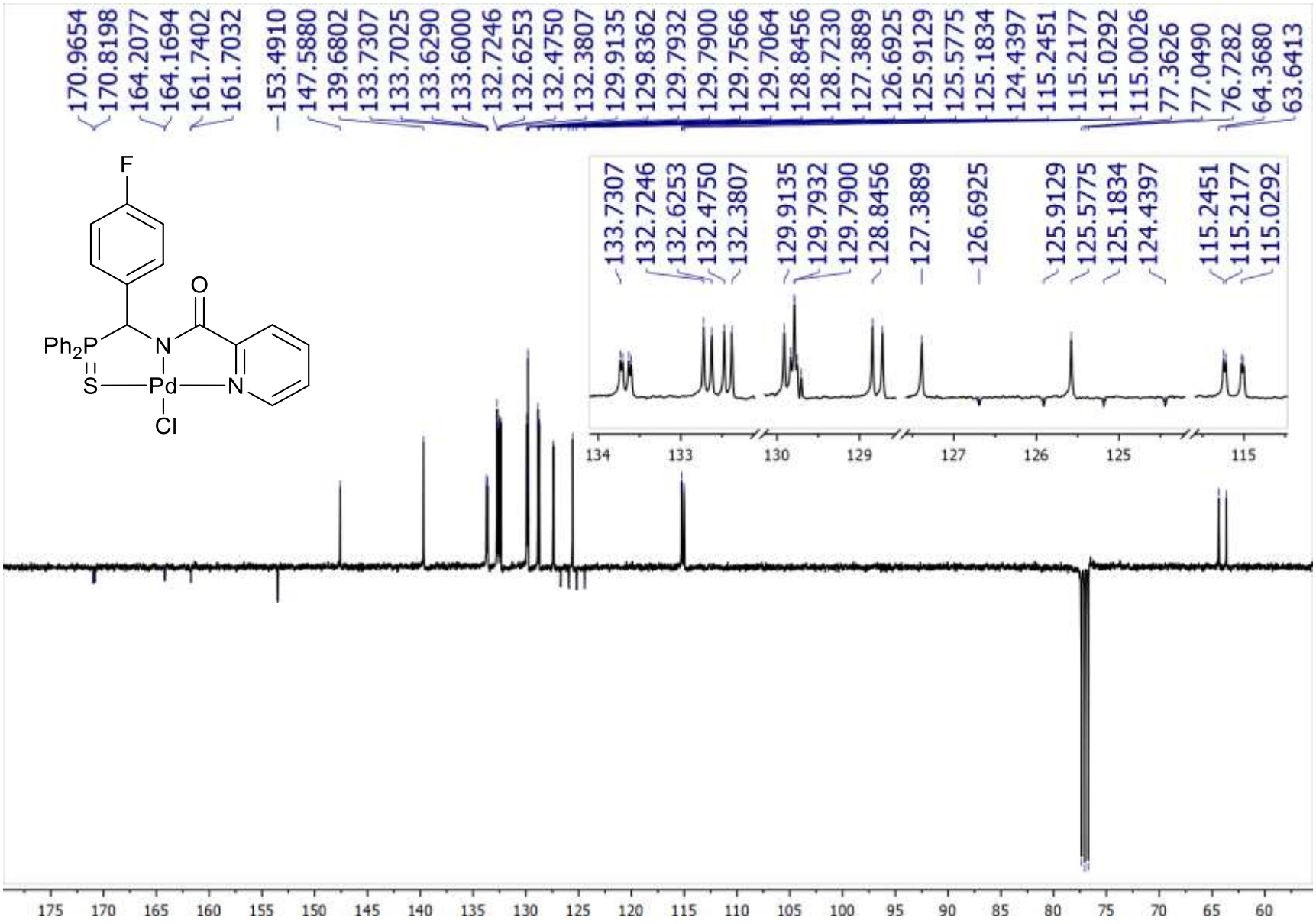

Figure S41. $^{13}C\{^{1}H\}$ NMR spectrum of complex **8d** (100.61 MHz, $CDCl_3$)

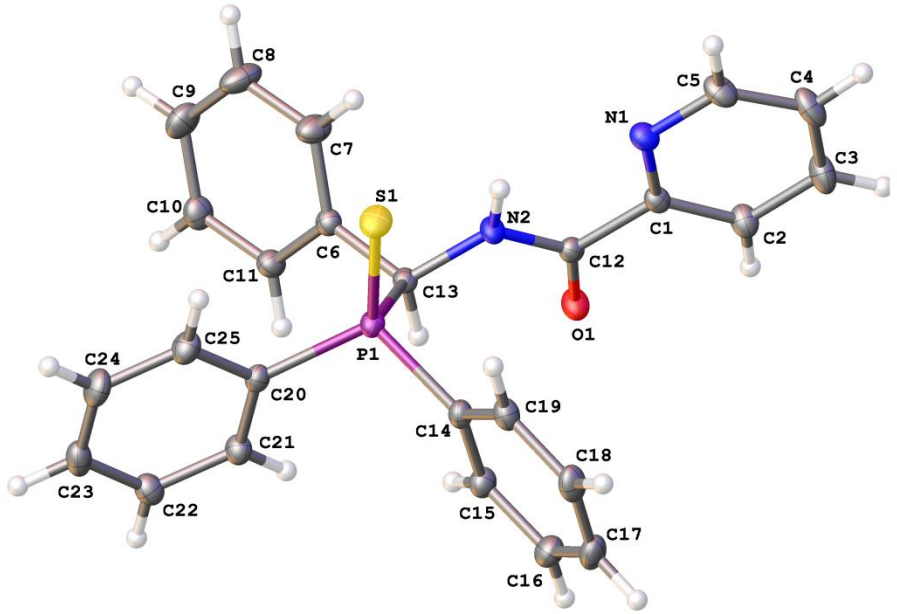

a

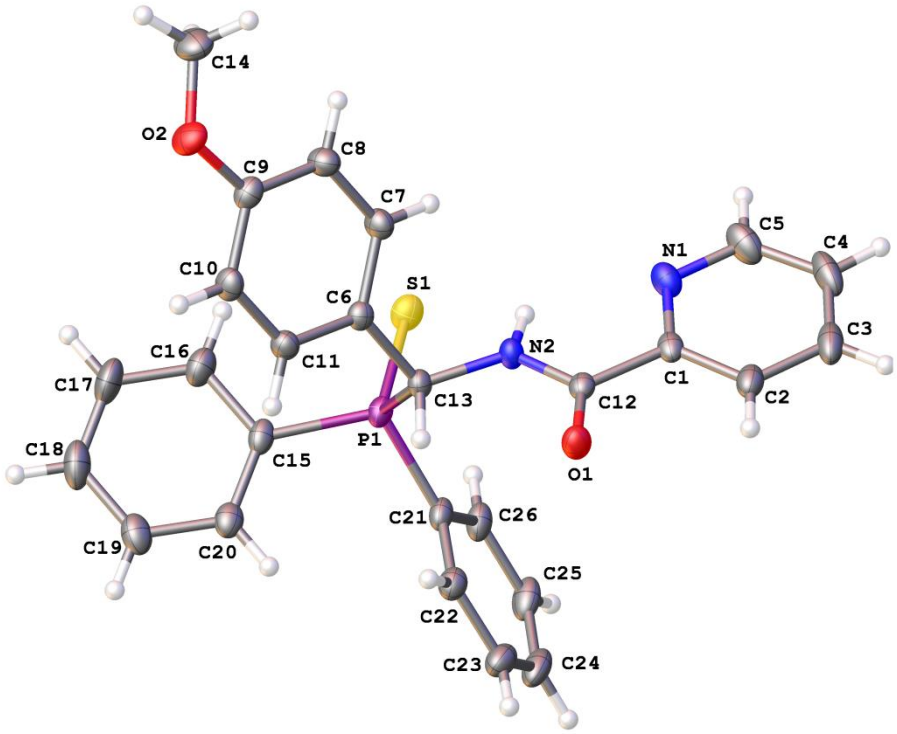

b

Figure S42. Molecular structures of ligands **6a** (***a***) and **6b** (***b***) in representation of non-hydrogen atoms as thermal ellipsoids at 50% probability level

Table S1. Selected bond lengths (Å) and angles (°) for compounds **6a,b**, **7**, and **8a**–**d**

	6a	**6b**	**7**	**8a**	**8b**	**8c**	**8d**
Pd1–Cl1	–	–	2.3127(6)	2.3122(4)	2.303(4)	2.2954(15)	2.3024(4)
Pd1–S1	–	–	2.3018(6)	2.2951(4)	2.297(3)	2.2960(15)	2.3003(5)
Pd1–N1	–	–	2.040 (2)	2.0401(12)	2.029(9)	2.027(5)	2.0361(15)
Pd1–N2	–	–	1.9913(19)	2.0000(12)	1.991(10)	1.993(5)	1.9854(14)
P1–S1	1.9540(4)	1.9595(5)	2.0197(9)	2.0175(5)	2.016(4)	2.007(2)	2.0139(6)
P1–C13(C7)[a]	1.8641(11)	1.8653(14)	1.803(2)	1.8479(14)	1.831(11)	1.847(6)	1.8448(17)
C13(C7)–N2[a]	1.4504(13)	1.4450(17)	1.460(3)	1.4629(17)	1.480(15)	1.471(7)	1.458(2)
N2–C12(C6)[a]	1.3427(14)	1.3411(17)	1.330(3)	1.3408(18)	1.344(14)	1.323(8)	1.341(2)
C12(C6)–O1[a]	1.2277(13)	1.2269(17)	1.242(3)	1.2375(17)	1.238(14)	1.236(7)	1.232(2)
C12(C6)–C1[a]	1.5034(14)	1.5021(18)	1.502(3)	1.5110(19)	1.476(16)	1.502(8)	1.503(2)
C1–N1	1.3393(14)	1.3392(19)	1.353(3)	1.3522(18)	1.364(15)	1.364(8)	1.348(2)
C1–C12(C6)–O1[a]	121.74(10)	122.24(12)	120.8(2)	120.68(12)	122.7(10)	120.4(5)	121.51(16)
O1–C12(C6)–N2[a]	124.03(10)	124.46(13)	126.9(2)	126.87(13)	124.8(10)	126.9(6)	125.92(16)
C13(C7)–P1–S1[a]	110.64(4)	110.27(5)	108.16(8)	106.90(15)	106.3(4)	106.4(2)	107.99(6)
N1–Pd1–S1	–	–	172.68(6)	172.49(3)	171.9(3)	171.89(15)	172.79(4)
N2–Pd1–Cl1	–	–	176.32(6)	176.20(3)	176.8(3)	177.19(15)	176.08(4)
N2–Pd1–N1	–	–	80.38(8)	80.85(5)	81.1(4)	81.0(2)	80.82(6)
N2–Pd1–S1	–	–	92.73(6)	91.74(3)	91.6(3)	92.01(14)	92.05(4)
S1–Pd1–Cl1	–	–	90.46(2)	91.331(14)	91.32(12)	90.41(5)	91.760(16)
Cl1–Pd1–N1	–	–	96.52(6)	96.02(4)	96.1(3)	96.47(15)	95.35(4)

[a] the bracketed atom numbers refer only to complex **7.**

X-ray crystallography

Single crystals of the compounds explored were obtained by slow crystallization from EtOAc–hexane (**6a**), $CHCl_3$–Et_2O (**7**), $CHCl_3$–hexane (**8a**), $CHCl_3$–CH_2Cl_2–Et_2O (**8b–d**) or slow recrystallization from EtOAc (**6b**). X-ray diffraction data were collected at 100 K with a Bruker Quest D8 CMOS diffractometer, using graphite monochromated Mo-Kα radiation (λ = 0.71073 Å). Using Olex2 [1], the structures were solved with the ShelXT structure solution program [2] using Intrinsic Phasing and refined with the XL refinement package [3] using Least-Squares minimization against F^2_{hkl} in anisotropic approximation for non-hydrogen atoms. The hydrogen atom of the NH group in ligands **6a,b** was located from difference Fourier synthesis, while the positions of the other hydrogen atoms were calculated, and they all were refined in isotropic approximation within the riding model. Crystal data and structure refinement parameters are given in Table S2.

Table S2. Crystal data and structure refinement parameters for compounds **6a,b**, **7**, and **8a–d**

Comp.	**6a**	**6b**	**7**	**8a**	**8b**	**8c**	**8d**
Empirical formula	$C_{25}H_{21}N_2OPS$	$C_{26}H_{23}N_2O_2PS$	$C_{19}H_{16}ClN_2OPPdS$	$C_{26}H_{21}Cl_4N_2OPPdS$	$C_{30}H_{32}ClN_2O_3PPdS$	$C_{27}H_{20}Cl_4N_3OPPdS$	$C_{26}H_{20}Cl_4FN_2OPPdS$
Formula weight	428.47	458.49	493.22	688.68	673.45	713.69	706.67
T, K	100	100	100	100	100	100	100
Crystal system	Triclinic	Monoclinic	Monoclinic	Triclinic	Monoclinic	Triclinic	Monoclinic
Space group	$P\bar{1}$	$P2_1/c$	$P2_1/c$	$P\bar{1}$	$P2_1/c$	$P\bar{1}$	$P2_1/c$
Z	2	4	4	2	4	2	4
a, Å	9.8186(3)	11.9627(3)	9.2430(11)	9.5575(4)	14.0537(11)	9.9279(7)	9.4217(3)
b, Å	10.1013(3)	19.9021(6)	10.5070(12)	11.4798(5)	11.5635(10)	12.9563(9)	15.3527(5)
c, Å	12.0509(3)	15.1273(4)	19.920(2)	13.1669(5)	19.5357(17)	13.4185(10)	19.3509(5)
α, °	104.5460(10)	90	90	88.1620(10)	90	103.396(4)	90
β, °	100.9210(10)	136.6532(10)	102.649(2)	70.7500(10)	110.681(4)	105.449(4)	95.3030(10)
γ, °	104.4390(10)	90	90	88.3500(10)	90	112.525(4)	90
V, Å^3	1079.09(5)	2472.14(12)	1887.6(4)	1362.92(10)	2970.2(4)	1424.69(18)	2787.10(15)
D_{calc} (g cm^{-1})	1.319	1.232	1.736	1.678	1.506	1.664	1.684
μ, cm^{-1}	2.44	2.20	13.31	12.32	8.73	11.83	12.13
F(000)	448.0	960	984.0	688	1376	712	1408
$2\theta_{max}$, °	56	56	58	58	50	54	56

Reflections measured	12846	30003	22342	17069	21534	15977	33648
Independent reflections	5164	5959	5020	7240	5220	6197	6733
Observed reflections [$I > 2\sigma(I)$]	4840	5187	4295	6687	5039	4926	6226
Parameters	271	290	235	344	384	343	334
R1	0.0298	0.0368	0.0294	0.0203	0.1059	0.0634	0.0246
wR2	0.0786	0.1041	0.0649	0.0499	0.2612	0.1976	0.0588
GOF	1.021	1.043	1.051	1.020	1.371	1.071	1.066
$\Delta\rho_{max}/\Delta\rho_{min}$ (e Å^{-3})	0.419/ –0.239	0.337/ –0.518	0.484/ –0.653	0.475/ –0.532	1.277/ –3.032	2.374/ –1.167	0.718/ –0.864
CCDC	2263286	2282340	2263287	2263288	2282342	2282343	2282344

References

1. O. V. Dolomanov, L. J. Bourhis, R. J. Gildea, J. A. K. Howard, H. Puschmann, OLEX2: A Complete Structure Solution, Refinement and Analysis Program, *J. Appl. Crystallogr*., **2009**, *42*, 339–341, DOI: 10.1107/S0021889808042726.
2. G. M. Sheldrick, SHELXT – Integrated Space-Group and Crystal-Structure Determination, *Acta Crystallogr. A: Found. Adv.*, **2015**, *71*, 3–8, DOI: 10.1107/S2053273314026370.
3. G. M. Sheldrick, A Short History of *SHELX*, *Acta Crystallogr*., *Sect. A: Found. Crystallogr*., **2008**, *64*, 112–122, DOI: 10.1107/S0108767307043930.

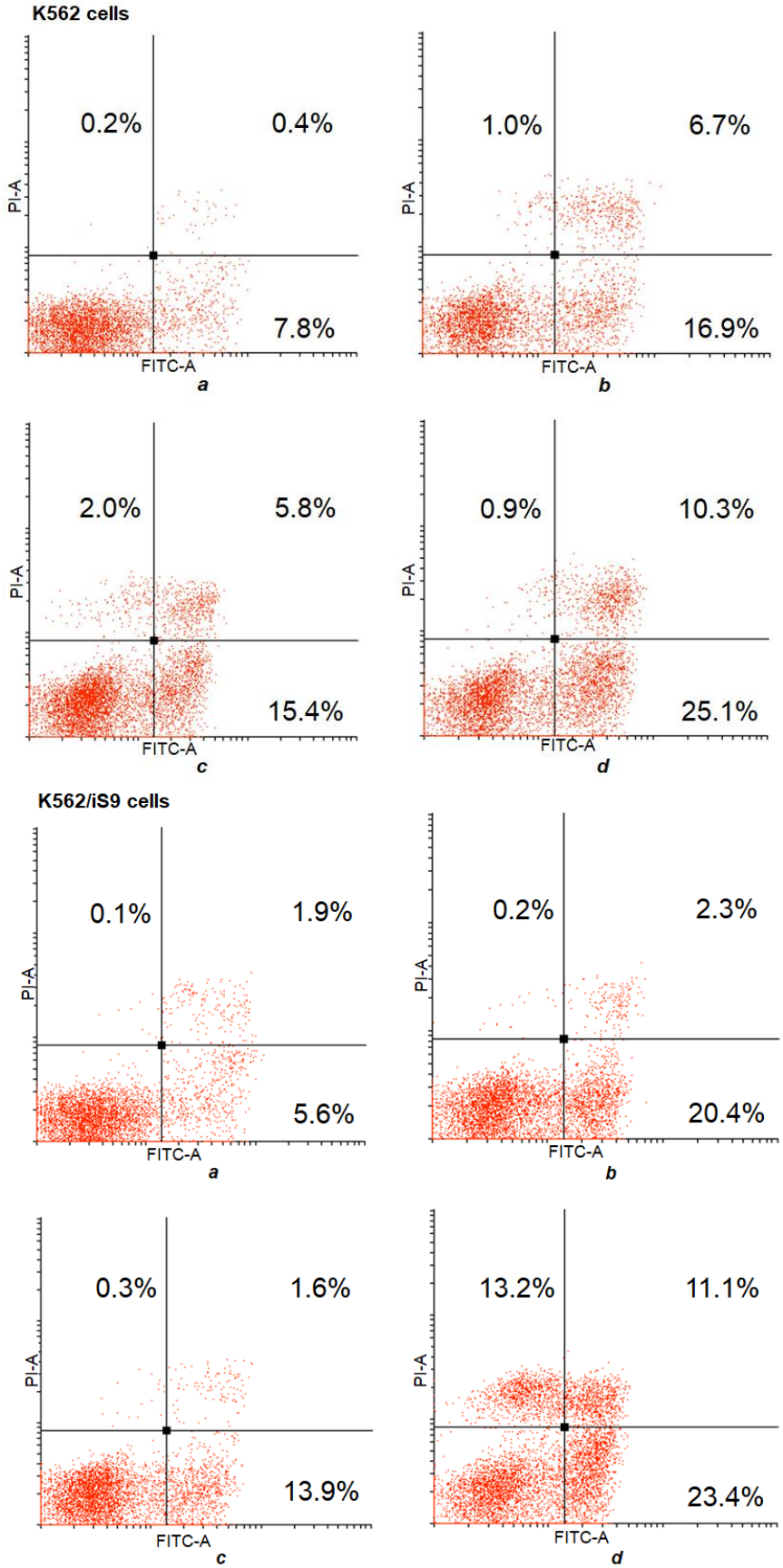

Figure S43. Percentages of necrotic (upper left quadrants), early apoptotic (lower right quadrants), and late apoptotic (upper right quadrants) K562 and K562/iS9 cells in the control experiments (***a***) and after exposure to complexes **8b** (***b***), **8c** (***c***), and **8d** (***d***) for 20 h